INVESTIGATIONS OF DETAIL DESIGN ISSUES FOR THE HIGH SPEED ACOUSTIC WIND TUNNEL USING A 60TH SCALE MODEL TUNNEL

by

P. S. Barna

Final Report

Contract #17GFY910191

* * * * * * * * *

Part II

Tests with the Closed Circuit

October 1991

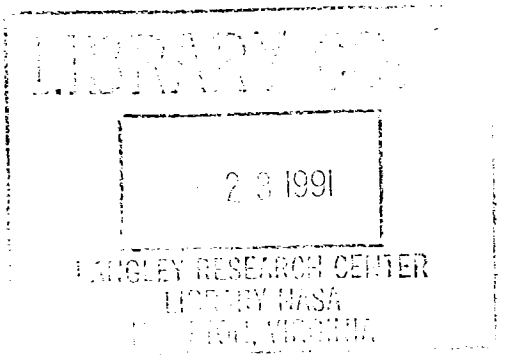

SCREEN IMAGE USER=*EBB SESSION=T20BR08 2/ 1/93-02:42:55-PM

DISPLAY 93N14738/2
93N14738*# ISSUE 4 CATEGORY 2
RPT#: NASA-CR-191672 NAS 1.26:191672 91/10/00 65 PAGES UNCLASSIFIED DOCUMENT
UTTL: Investigations of detail design issues for the high speed acoustic wind tunnel using a 60th scale model tunnel. Part 2: Tests with the closed circuit TLSP: Final Report
AUTH: A/BARNA, P. STEPHEN
CORP: Barna (P. Stephen), Consultant, Norfolk, VA.
SAP: Avail: CASI HC A04/MF A01
CIO: UNITED STATES
MAJS: /*AEROACOUSTICS/*FLOW DISTRIBUTION/*SCALE MODELS/*TURBOFANS/*WIND TUNNEL TESTS
MINS: / AIR FLOW/ AXIAL FLOW/ DIFFUSERS/ NOZZLES/ POSITION (LOCATION)/ TEST CHAMBERS
ABA: Author
ABS: This report summarizes the tests on the 1:60 scale model of the High Speed Acoustic Wind Tunnel (HSAWT) performed during the period June - August 1991. Throughout the testing the tunnel was operated in the 'closed circuit mode,' that is when the airflow was set up by an axial flow fan, which was located inside the tunnel circuit and was directly driven by a motor. The tests were first performed with the closed test section and were subsequently repeated with the open test section, the latter

ENTER: MORE

DISPLAY 93N14738/2

operating with the nozzle-diffuser at its optimum setting. On this subject, reference is made to the report (1) issued January 1991, under contract 17-GFY900125, which summarizes the result obtained with the tunnel operating in the 'open circuit mode.' The tests confirmed the viability of the tunnel design, and the flow distributions in most of the tunnel components were considered acceptable. There were found, however, some locations where the flow distribution requires improvement. This applies to the flow upstream of the fan where the flow was found skewed, thus affecting the flow downstream. As a result of this, the flow appeared separated at the end of the large diffuser at the outer side. All tests were performed at NASA LaRC.

ENTER:

INVESTIGATIONS OF DETAIL DESIGN ISSUES FOR THE HIGH SPEED ACOUSTICS WIND TUNNEL USING A 60th SCALE MODEL TUNNEL

by

P.S. Barna

Part II. Tests With the Closed Circuit

Contract # 17-GFY910191

October, 1991.

SUMMARY

This report summarizes the tests on the 1:60 scale model of the High Speed Acoustic Wind Tunnel (HSAWT) performed during the period June - August 1991.

Throughout the testing the tunnel was operated in the "closed circuit mode," that is when the airflow was set up by an axial flow fan, which was located inside the tunnel circuit and was directly driven by a motor.

The tests were first performed with the closed test section and were subsequently repeated with the open test section, the latter operating with the nozzle-diffuser at its optimum setting. On this subject, reference is made to the report [1] issued January 1991, under contract 17-GFY900125, which summarizes the result obtained with the tunnel operating in the "open circuit mode."

The tests confirmed the viability of the tunnel design, and the flow distributions in most of the tunnel components were considered acceptable. There were found, however, some locations where the flow distribution requires improvement. This applies to the flow upstream of the fan where the flow was found skewed, thus affecting the flow downstream. As a result of this, the flow appeared separated at the end of the large diffuser at the outer side.

All tests were performed at NASA Langley Research Center.

TABLE OF CONTENTS

INTRODUCTION

The underlying idea behind the open circuit was two-fold: economy and exigency. For one, the procurement and installation of a commercial centrifugal blower, employed to induce the flow around the open tunnel circuit, proved economical and its operation proved simple: to set the fan rotating, all that was required was to throw the switch in the electric power line. No other, than the person taking the readings, was needed. The closed circuit operation proved more complex. For the other, the operation of the tunnel was enhanced by the various changes in the experimental set-up, which could be rapidly and economically produced during a relatively brief period. Since time was also an essence of the contract, the most relevant results could be obtained over a period of about six months.

Furthermore, the results obtained could be ultimately employed for guidance to the more complete closed circuit, which was planned to follow the open circuit operation. Thus the results obtained from the open circuit were used:

1. to establish the flow patterns and the pressure distribution around the circuit;
2. to estimate the future axial flow fan power;
3. to open the way and lead to component optimization.

Thus the open circuit operation could be considered of exploratory nature, basic to the closed circuit testing. Subsequently, the closed circuit tunnel became more representative of the prototype [2], than the open circuit tunnel was for preliminary testing.

For the closed circuit operation, the relevant corners, previously turned outwardly were returned to form the closed loop. The fan section, formerly fitted with a simple nacelle was replaced by an axial flow fan specially designed to meet the same flow rate as obtained earlier with the use of the centrifugal blower.

Last, but not least, the open and closed circuit operation enabled the observers, by comparing results, to establish the difference - if any - between the data obtained with the different circuits possibly leading to improvements.

BRIEF DESCRIPTION OF THE MODEL TUNNEL

The basic floor plan for the closed return circuit model tunnel is shown in figure 1, where the various components are recognized as follows:

1. Test section (either closed or open);
2. First diffuser;
3. First corner;
4. First cross leg;
5. Second corner;
6. Fan section (complete with fan and motor);
7. Distancing spool;
8. Second (large) diffuser;
9. Third corner;
10. Second cross leg, fourth corner;
11. Wide angle diffuser;
12. Cooling radiator for recirculating air;
13. Calming chamber with honeycomb;
14. Contraction.

Materials: the ducts were made of fiberglass and of plexiglass, the nacelles of wood and the casing around the fan was 0.5 ins. thick aluminum. It is noted that the addition of the cooling system increased the length of the first leg by about 2 inches; this was compensated by lengthening the fan section by the same amount. After the installation of the open test section, the application of an additional spool in the second leg became necessary, because the length of the open test section proved to be longer than that of the closed test section. While operating with the open test section this spool was located upstream from the fan section. A narrow air-gap was provided between the end of the large diffuser and the third corner for ventilation. Figure 2 shows a view of the model tunnel.

The Fan Section

The fan section included the axial flow fan, the drive motor, the downstream guide vanes, the up- and downstream nacelles and cooling ducts for the electric motor. Details of the internal arrangement of the fan section is shown in figure 3(a), where the various components are labeled and are listed for convenience. Figure 3(b) is a view of the assembly.

The axial flow fan was designed to discharge about 27.5 cubic feet per second against a static pressure rise of 32.5 psf for standard air when rotating at 11,650 rpm. The fan had 12 blades of length 1.375 ins., with an outside diameter of 8.50 ins. and hub diameter 5.75 ins., as shown in figure 4. The profile of the blades were Clark Y 12.5% thick with a chord of constant 1.25 ins. The material employed was aluminum 7075-T6, with a yield stress of 72,000 psi. The rotor was dynamically balanced. There were 17 downstream guide vanes employed both for straightening the flow and for supporting the fan and motor. Figure 5 shows the guide vanes from the rear.

The drive for the fan was a 2 H.P. electric motor operating on 200 Volts and 400 Hz. frequency. The motor was properly grounded. Cooling of the motor was obtained with a cross-current air supply described in detail in ref. 1. The supply of air was arranged through a pressure reducer with a 6 ft. long and 1/4 inch I.D. airline between the reducer and air inlet to the motor and the source was the standard high pressure workshop air facility.

Cooling of the tunnel air was attained by the installation of a standard motor car radiator (Ford Bronco 1983 V6) which was located between the exit from the wide angle diffuser and the inlet to the calming section. The cooling medium was tap water with a flow rate of about 1 gallon per minute. To avoid damage to the radiator core, both sides were covered with a 1/4 inch plate extending right across the total face area and having a 13.5 ins. diameter hole for air passage.

For measuring temperatures, thermocouples were employed and they were located at relevant points. One thermocouple measured the rise in temperature of the motor itself, while others established temperatures of the outgoing water, air inside the tunnel and fan cooling air, at exit.

Electric power was obtained from a generator located outside the laboratory. The rotational speed (rpm) of the motor was established electronically.

METHOD OF EXPERIMENTS

Safety Measures

Prior to the tests, precautionary safety measures were introduced.

a. The fan assembly was tested in order to establish its natural frequency. In addition, the fan also underwent a series of "shake-down" runs while instrumented with accelerometers. Analysis of the data obtained led to motor speed for the aerodynamic testing.

b. The noise level of the tunnel was measured under actual operational conditions.

c. The blade disc was X-rayed and found to be free of cracks.

d. The use of either city water or a closed-loop system was studied for the cooling of the tunnel air.

e. Operating procedures were prepared.

The natural frequency was established during the shakedown tests, when accelerometers were initially employed while the fan was increasing its speed. Noise level was measured with a sound level meter. Upon deciding the use of city water, a solenoid valve was installed in the electric circuit which enabled the water flow to be stopped immediately after the current to the motor was shut off. Furthermore, alarms were introduced to monitor and to control: the rise in motor temperature, limited to 210 deg. F; the temperature rise of the air and of the cooling water, respectively. The high pressure air line for cooling the motor was equipped with a pressure reducer and shut-off valve.

The electric power line plan (figure A-I) and the operating procedures are shown in APPENDIX A.

Aerodynamic Test Methods

As before [1], a single electronic pressure gauge was used for taking both, velocity traverses and measuring pressures. A manually operated scanning valve was employed to monitor the static pressures at various locations. The static pressure ports were also employed for reading the static part of a pitot-static differential for the velocity traverses. Various pitot tubes were used for measuring total pressures and these were inserted into the stream through small openings in the tunnel wall. All measurements were taken under steady flow conditions, while running the motor at a constant speed of about 10,970 rpm. Horizontal velocity traverses were obtained at locations #1 to #14 (except #9 at the fan location), while vertical traverses were taken at location #4 and #6. In the high velocity locations the pitot tube was replaced by a pitot-cylinder, consisting of a long 1/8 inch diameter tube provided with a small port facing the stream. During the traversing, the tube remained extended across the section-being at least twice as long as the section under consideration. This was done in order to avoid skewing the profiles which is generally experienced during the gradual withdrawal of a standard Pitot tube while traversing the stream. Prior to the tests the electronic pressure gauge was calibrated.

Briefly, each testing "run" required - in addition to the experimenter - two persons from the workshop of the Acoustic Laboratory. One person was monitoring the electric power and the other was handling and monitoring the various devices located near the model tunnel. These two persons communicated with each other.

It appeared during the tests, that the motor was running hot already about 10 minutes after start, so that the tests had to be performed at an accelerated pace. Apparently, the power of the motor was greater than the power absorbed by the fan. To allow for an adequate cooling-off, a period of about half and hour was required prior to engaging in the next run. Typical heating up curves are shown in the APPENDIX B, where the temperature of the motor is plotted against time in minutes. (Figure B-1)

It is of some interest to note, that the noise generated by the fan itself appeared a high pitch hum, quite tolerable at that. Vibration of the fan, even at the highest speed, was negligible. Since, however, the motor cooling air line had a small diameter, 0.25 ins., the exiting air created an additional hissing noise which proved rather unpleasant.

RESULTS WITH THE CLOSED TEST SECTION

Horizontal traverses

Traverses in the horizontal plane are presented in figure 6, where the normalized velocity V/V_{ave} is plotted against normalized travel distance x/w. (Note: in the earlier reports, the normalized velocity was V/V_{max}, where V_{max} was the maximum flow velocity attained at the cross section under consideration. However, V_{max} varied a great deal and therefore it was subsequently replaced by V_{ave} derived from the flow rate Q upon dividing it with the area of the section).

Figure 6a shows the traverse at location #1 downstream from the fourth corner and the "humps and hollows" in the distribution signify the effects of the turning vanes on the flow. Between x/w=0.3 and 0.85 one finds V/V_{ave} as being rougly one, while near the extremities it is above one, thus giving the impression that V_{ave} is too low. This may not be the case, however, when considering the vertical distribution which may compensate for these effects.

At location #2, at inlet to the contraction, one observes the opposite effect: V_{ave} may be found too high, because the distribution appears to be somewhat below one, as shown in figure 6b. The uneven distribution is rather disappointing when considering that this location is downstream from the radiator, honeycomb and the screen.

At location #3, at exit from the contraction, the flow distribution appears in figure 6c to be perfectly uniform and seems to be free of the irregularities in the flow experienced upstream. This result signifies, that the contraction is a satisfactory design.

At exit from the closed test section, that is at the inlet to the first diffuser, location #4, there appears a small boundary layer build-up, while the "core-flow" remains uniform, as shown in figure 6d. Further along the first diffuser, at location #5, the boundary layer build-up amounts to about 20 percent, as shown in figure 6e, while at exit from the first diffuser, location #6, the boundary layer build-up is about 25 percent on each side as shown in figure 6f. Thus the build-up over the second part of the diffuser is less marked than over the first part.

Downstream from the first corner, location #7, the flow distribution appears slightly skewed and the boundary layer build-up on the inner side seems smaller, say 20%, than on the outer side, where it is about 35% thick, as shown in figure 6g. At the same time, one may also observe that the uniform part of the distribution is disturbed, and a peak appears at x/w=0.64. These effects may be caused by turning vane imperfections.

Downstream from the second corner, location #8, the flow distribution becomes much worse. The uniform part of the distribution could no longer be observed and the peak moved inboard to x/w=0.26. Over the outer region, say, between x/w=0.64 and 1.0, a marked slowing of the flow may be observed, as shown in figure 6h. While some of these effects may be caused by some turning vane imperfections, questions also arise about other, yet unknown effects, as well.

Downstream from the fan section, at locations #10 and #11, the familiar velocity defect over the center region may be observed, which decreases in "depth", as shown in figures 6i and 6j. Surprisingly, the peak values observed do not differ a great deal, being about 1.1 at the inner and about 1.05 at the outer region at location #11.

In going further downstream, however, the flow distribution rapidly deteriorated. At location #12, the symmetry of distribution was disturbed by the rapid fall of velocity in the outer region and there could be separation of the flow as indicated by figure 6k, where V/V_{ave}= 0.156 was recorded at x/w=0.965, this being the last point of observation.

At the exit end of the large diffuser, at location #13, effects of the third set of turning vanes became noticeable, as shown in figure 6ℓ. Apparently, as the flow began to turn it picked up speed near the inner region only to further slow down in the outer region. When compared with figure 6k, where the fall-off began at x/w=0.68, it already starts at 0.6, shown in figure 6ℓ.

Consider for a moment the location of the spool. When the spool was located upstream of the fan section, that is, between the second corner and entry to the fan section, the results obtained are as shown in figure 6ℓ. When, however, the spool was relocated downstream from the fan, that is between entry to the large diffuser and the exit from the fan section, the results improved. This is shown in figure 6m which differs from 6ℓ. As a matter of fact, there is a noticeable improvement, the curve ends around 0.55, instead of 0.2, which is gratifying. There is a lesson that could be learned from this effect.

Downstream from the third corner, at location #14, two peaks appear in the flow distribution, one inboard and the other outboard, figure 6n. In between these two peaks, a large part of the flow appeared near $V/V_{ave}=1$, given + or - 0.5, thus indicating that the flow had a tendency to be straightened out to some extent. The distribution at location #1 (already presented) seems similar, except for the usual "humps and hollows" which are due to the influence of the turning vanes.

Vertical traverses with the test section closed

Results of the vertical traverses are shown in figure 7. When compared with the horizontal traverses, the results are about the same. At location #3, at inlet to the test section, the flow was found perfectly uniform, as shown in figure 7a, while at location #4, a small build-up of the boundary layer became noticeable, as shown in figure 7b.

At exit from the first diffuser, at location #6, the vertical distribution also appeared similar to that found with the horizontal, having a uniform "core", as shown in figure 7c. These effects are usually considered normal.

Pressure distribution with the test section closed

The pressure distribution is presented in figure 8, where the subatmospheric pressure, Pa - P (psf), is plotted against tunnel location. The diagram clearly shows the static pressure changes around the tunnel, which differs in two aspects from that presented in the report on the open circuit [1], namely: there appears no longer a pressure build-up over the closed test section owing to improvements made in pressue ports and there is an axial flow fan in the closed circuit, an additional feature.

It is noted that the static pressure rise along the fan section is somewhat less than the design total pressure rise owing to the losses experienced along the fan section. Also, consideration must be given to the difference between the design rotational speed, 11,650 rpm, and the actual test speed, 10,970 rpm. At this rotational speed the flow rate was found to be 25.84 cuft/second. The tests have also shown, that after the necessary corrections were made for the speed difference, the flow rate obtained with the axial flow fan closely agreed with the design rate, namely 27.5 cuft/per second.

The static pressure recovery in the first diffuser was found to be 62.7 percent, and in the large second diffuser 65.45 percent of the average kinetic energy prevailing at diffuser entry. These results compare well with figures published in the DIFFUSER DATA BOOK [3]. Details of the calculations are shown in APPENDIX C.

Based on static pressure changes, the loss coefficient of the first corner was 0.204, while the second corner was 0.309 when using the Salter vane design. Details of the calculations are shown in APPENDIX D. Results on the first corner agree reasonably well with data in the literature [4], especially when consideration is given to the low Reynolds numbers obtained in the model tunnel. However, results on the second corner were found considerably higher, which is consistent with the data obtained with the open circuit.

The results presented above were obtained with the first and second corners fitted with the Salter type vanes [5]. For more details on turning vane design, see also Ref. 1.

RESULTS WITH THE OPEN TEST SECTION

Horizontal traverses

Traverses in the horizontal plane are presented in figure 9. In general, the flow rate with the open test section proved about 5 percent less than with the closed test section.

Figures 9a and 9b, representing the flow distribution at locations #1 and #2, respectively, show little if any difference between the open and closed test section, the reason being, that these are upstream from the test section. Inside the open test section, location #3 was the exit plane of the nozzle-diffuser which was fully described in Ref. 1. Because of the diffusion effects, the average exit velocity from the nozzle-diffuser decreased by about 24% from the velocity experienced in the closed test section. However, the flow distribution remained uniform across the stream with only a small, about 5% build-up in the boundary layer, as shown in figure 9c.

At entry to the first diffuser, at location #4, the uniform distribution narrowed somewhat owing to the build-up of the boundary layer, now amounting to about 10% as shown in figure 9d. This build-up was produced by the presence of the collector, which was also described in Ref. 1.

Further downstream along the first diffuser, at location #5, the distribution changes to non-uniformity, having two "humps" and one "hollow", shown in figure 9e. This raises the questionability of the collector design and the problem will be subject to further discussion later. At exit from the first diffuser, location #6, the distribution has a similar shape to that experienced at location #5, as shown in figure 9f. Similar remarks apply to the flow downstream from the first corner, location #7, as shown in figure 9g.

At locations #5, #6 and #7, the flow distribution is close to being symmetrical. However, downstream from second corner, location #8, the symmetry ends and the flow became distorted, as shown in figure 9h. A similar flow distribution was experienced with the closed test section (figure 6h), with the exception that the V/V_{ave} values are slightly different.

Downstream from the fan section, at locations #10, #11 and #12, the flow distributions were also found similar in shape and the figures 9i, 9j and 9k compare favorably with 6i, 6j and 6k. At the exit from the large diffuser, location #13, the flow distribution again became skewed and flow separation at outer wall was experienced, as shown in figure 9ℓ. It appears that the additional spool, placed upstream from the fan section, had an adverse effect on the flow distribution.

Downstream from the third corner, location #14, the flow distribution again exhibited two "humps", one inboard and the other outboard with an almost linearly decreasing "hollow" extending over half the width of the section, shown in figure 9m. In the future, subject to some modifications upstream, this distribution could become quite acceptable.

Vertical traverses with the open test section

Vertical traverses obtained at the inlet and exit of the first diffuser are shown in figure 10. The distributions exhibit altogether different characteristics from those experienced with the closed test section. They have a dome like shape and do not prove to be symmetrical. In particular, at inlet, location #4, V/V_{ave} rises from 0.72 to 1.12, off center, then decreases gradually to 0.78, as shown in figure 10a. At the exit from the first diffuser, the distribution became even more "domey", rising from 0.52 to 1.08 and decreasing to 0.48, as shown in figure 10b.

When considering the horizontal and vertical distributions, there appears a connection between the two in form of a flow adjustment. When the horizontal distribution at location #5 is compared with the vertical at #4, one realizes the flow adjustment: the hollow in the horizontal is compensated by a hump (dome-like) in the vertical, and vice versa.

Pressure distribution

Pressure distribution around the closed circuit, employing the open test section, is shown in figure 11. It appears that a large pressure loss, 10.98 psf, was experienced inside the open test chamber (surrounding the open test section). Accordingly, the flow rate decreased from 25.84 cuft/sec to about 24.47 cuft/sec, amounting to a drop of about 5 percent. The fan increased its static pressure rise to 33.3 psf at the fan speed of 10,970 rpm.

The static pressure recovery in the first diffuser was found to be 67.7 percent and in the second, large diffuser, 64.75 percent of the average kinetic energy prevailing at diffuser entry. For details of the calculations see APPENDIX C.

Based on static pressure changes, the loss coefficient of the first corner was 0.327, while the second corner was 0.3065, while using the Salter vane design. It is of interest to note that with the open test section, the first corner showed a higher loss that the second corner, quite a reverse to that experienced with the closed test section. The increase in the first corner loss while operating with the open test section is probably due to the unfavorable flow distribution upstream from the corner.

REVIEW OF DATA

Some of the relevant data recorded during the tests is shown in Table I. For both the closed and the open test section, static pressures P_2, P_3, flow rate Q and the average section velocity V_{ave} is shown for traverse locations from 1 to 14 together with the section areas and travel distances of the pitot tubes. Table I is shown as figure 12.

DISCUSSION OF THE RESULTS

Studying the performance of the model tunnel as a whole, one finds some parts of the tunnel which seem to work rather well while other parts need improvements. Furthermore, there appears a need for major and minor modifications as well.

With the closed test section, one finds the flow emerging from the contraction and the distribution in the test section itself, quite satisfactory. Recovery in the first diffuser and the flow distributions seemed up to standard requirement, while the flow emerging from the first corner appeared also acceptable. There appears to be no need for concern for the operation of these components when employing the closed test section.

With the open test section, one also finds the flow emerging from the contraction and distribution in the test section itself, quite satisfactory. However, while recovery in the first diffuser appeared acceptable, the flow distribution along the diffuser's length needs attention. The suspected component this time is the collector which must have an influence on the flow downstream. The collector needs further attention and may need minor modifications. It is suspected that the top/bottom and the side angles are perhaps too large.

Major modifications concern the turning vanes in the first and second corners. In particular, the turning of the flow by exactly 90 degrees was not obtained after the tunnel was first tested, and the application of trailing edge flaps became necessary. However, adjusting these flaps proved a laborious and time consuming experience. Fine tuning for the correct flow alignment would require a set of flow control vanes to be located in the first cross-leg, that is between the first and second corners, which could be manipulated from the outside until optimum flow was attained downstream. The tests showed that the flow distribution in the first cross leg markedly affected the distribution downstream from the second corner, resulting in a skewed distribution entering the fan section. As a result of this, the performance of the fan and the flow in the second (large) diffuser was adversely affected, resulting in such a poor distribution towards the exit of the large diffuser that flow separation was suspected. It is noted, that moving of the spool downstream from its upstream location of the fan section seemed to moderate the flow distribution at the exit from large diffuser, which is of considerable interest.

Minor modifications also concern the flow distributions downstream from the third and particularly from the fourth corner, whence the stream passes into the wide-angle diffuser. While the third corner seemed to straighten out the distribution to some extent, downstream from the fourth corner, large "humps and hollows" were observed, which were not removed adequately by the honeycomb, screen and the radiator (core). These shortcomings may be removed by simply replacing the Dimmock type vanes with the Salter design both in the third and in the fourth corner. If the flow at entry to the contraction would still remain unsatisfactory, the introduction of additional screens may become necessary. In addition, some study of the flow inside the wide angle diffuser may also be required.

CONCLUSIONS

Tests were performed on the 1/60 scale model of High Speed Acoustic Wind Tunnel operating with the closed circuit, which was provided with an axial flow fan for producing and maintaining the flow around the tunnel circuit.

The investigations showed, that:

1. The flow distributions in the first leg of the circuit proved satisfactory for the closed test section; for the open test section, minor modifications of the collector may become necessary in order to improve the flow distribution in the first diffuser.

2. Pressure recovery proved satisfactory in 1st and 2nd diffusers.

3. The flow downstream from the second corner became skewed so that the flow distribution into the fan became non-uniform around its circumference.

4. The flow downstream from the fan section remained skewed resulting in an undesirable flow distribution at the exit end of the second (large) diffuser.

5. The flow distribution downstream from the fourth corner proved unsatisfactory as the large turning vanes of the Dimmock design produced large wakes resulting in non-uniform flow which persisted right up the entrance to the collector.

6. The fan performed satisfactorily and for considerations of safety, it turned at 10,970 rpm instead of the design speed of 11,650 rpm.

RECOMMENDATIONS

It is recommended to extend the studies on turning vanes in order to improve the flow downstream, considering that the flow upstream is non uniform as experienced in closed circuit wind tunnels. Consideration may also be given to re-designing the section just upstream of the fan section in order to improve the flow distribution into the fan. Introduction of adjustable flow control vanes may also be considered.

To improve the flow downstream from the third and fourth corners a change over from the Dimmock to the Salter vane design may be considered as necessary. The introduction of additional screens may also become necessary.

In order to improve the flow distribution in the first diffuser while operating with the open test section, some variation in the side angles of the collector may prove helpful.

The rapid warming of the fan drive motor needs some consideration in future.

REFERENCES 3

1. Barna, P.S. : Investigations of detail design issues for the High Speed Acoustic Wind Tunnel using a 60th scale model. Part I. Tests with Open Circuits. March 1991. Contractor's report #17-GFY900125.

2. Prelimary Engineering Study for a High Subsonic Acoustic Wind Tunnel. Report issued by SVERDRUP TECHNOLOGY INC. August 1989. Contract # NAS1-18881 (A-E).

3. Rundstadler, P.W., et al.: Diffuser Data Book. TN-186, by CREARE LTD. May 1975.

4. Patterson, G.N.: Note on the design of corners in duct systems. R. & M. No. 1773 of G.B. October 1936.

5. Salter, C. : Experiments on thin turning vanes. R. & M. No. 2469, of G.B., 1946.

SYMBOLS

A	area, sq ft
c	specific heat, Btu/lb/°F
L	length, ft.
M	Mass, lb.
p	static pressure lb/ft^2
pt	total pressure, lb/ft^2
q	dynamic head, $1/2\ \rho\ V^2$, lb/ft^2
Q	heat, Btu
t	time, hr.
S	surface area, ft^2
V	velocity, ft./sec.
W	electric heat energy, Watts
W	massflow, lb/jr
x	horizontal distance, ft.

Abrreviations

HP	horsepower
Btu	british thermal unit
Hz	frequency, Herz
rpm	revolution per minute
Re	Reynolds number

Greek letters

α	heat transfer coefficient, Btu/hr, deg F, ft^2
δ	boundary layer thickness
ρ	density, $slugs/ft^3$
ν	kenematic viscosity, ft^2/sec
η	efficiency in recovery
θ	static temperature, °F

Subscript

ave	average
max	maximum

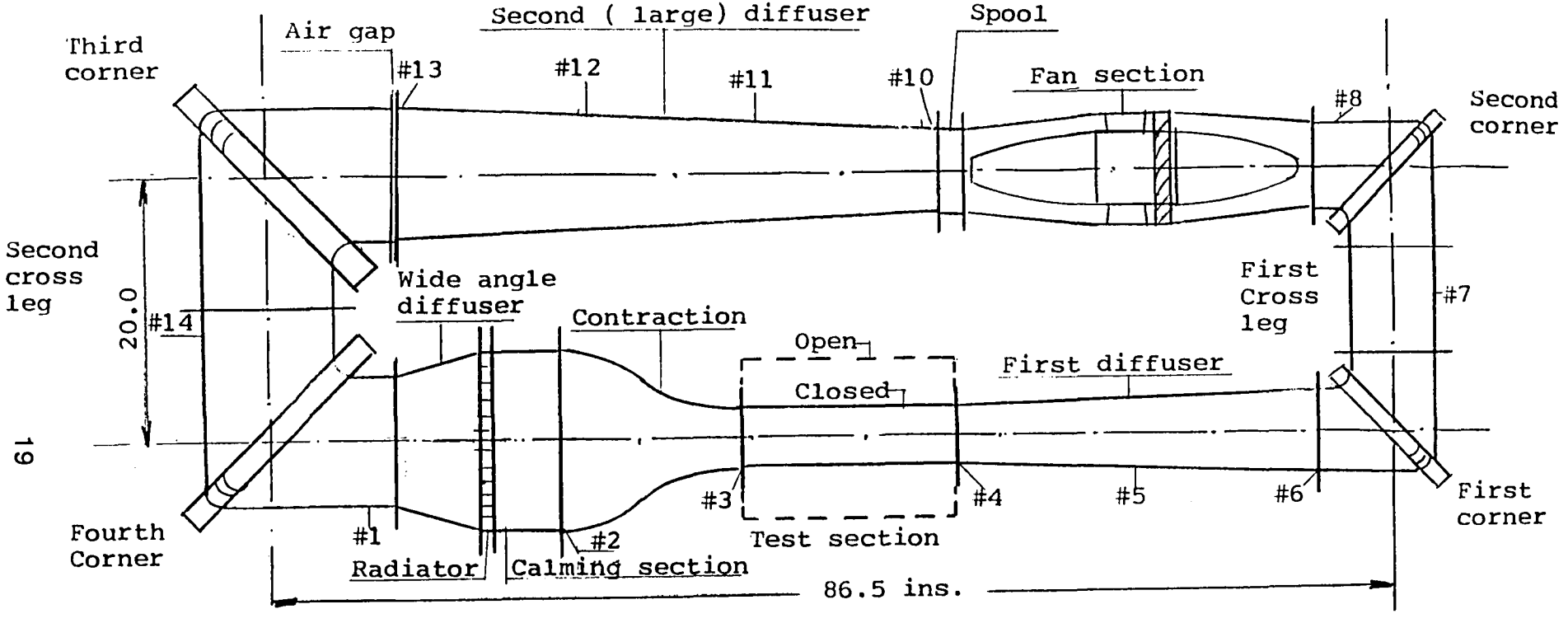

Figure 1. Basic floor plan of the closed return circuit model tunnel
(Numbers refer to traverse locations)

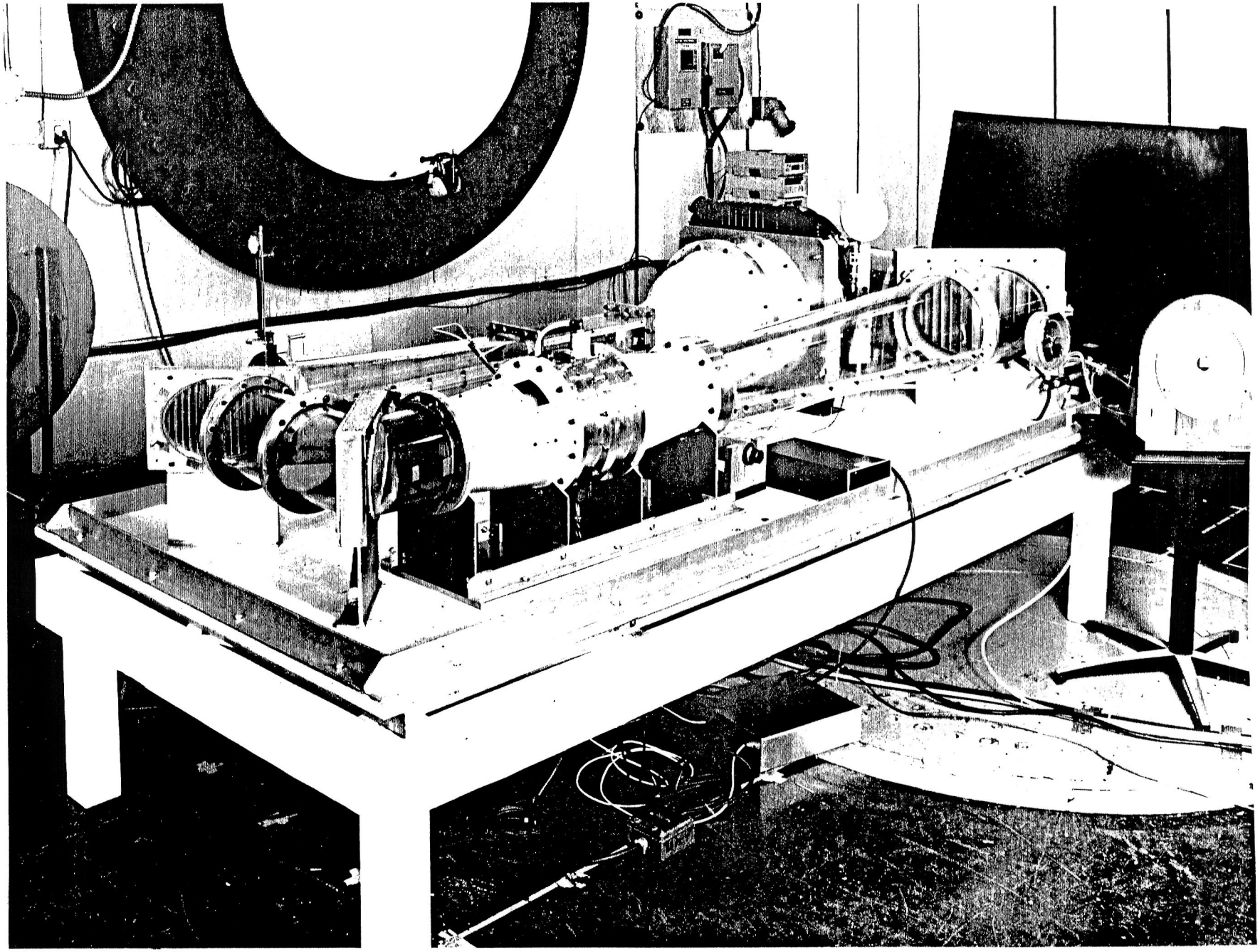

Figure 2. View of the model tunnel

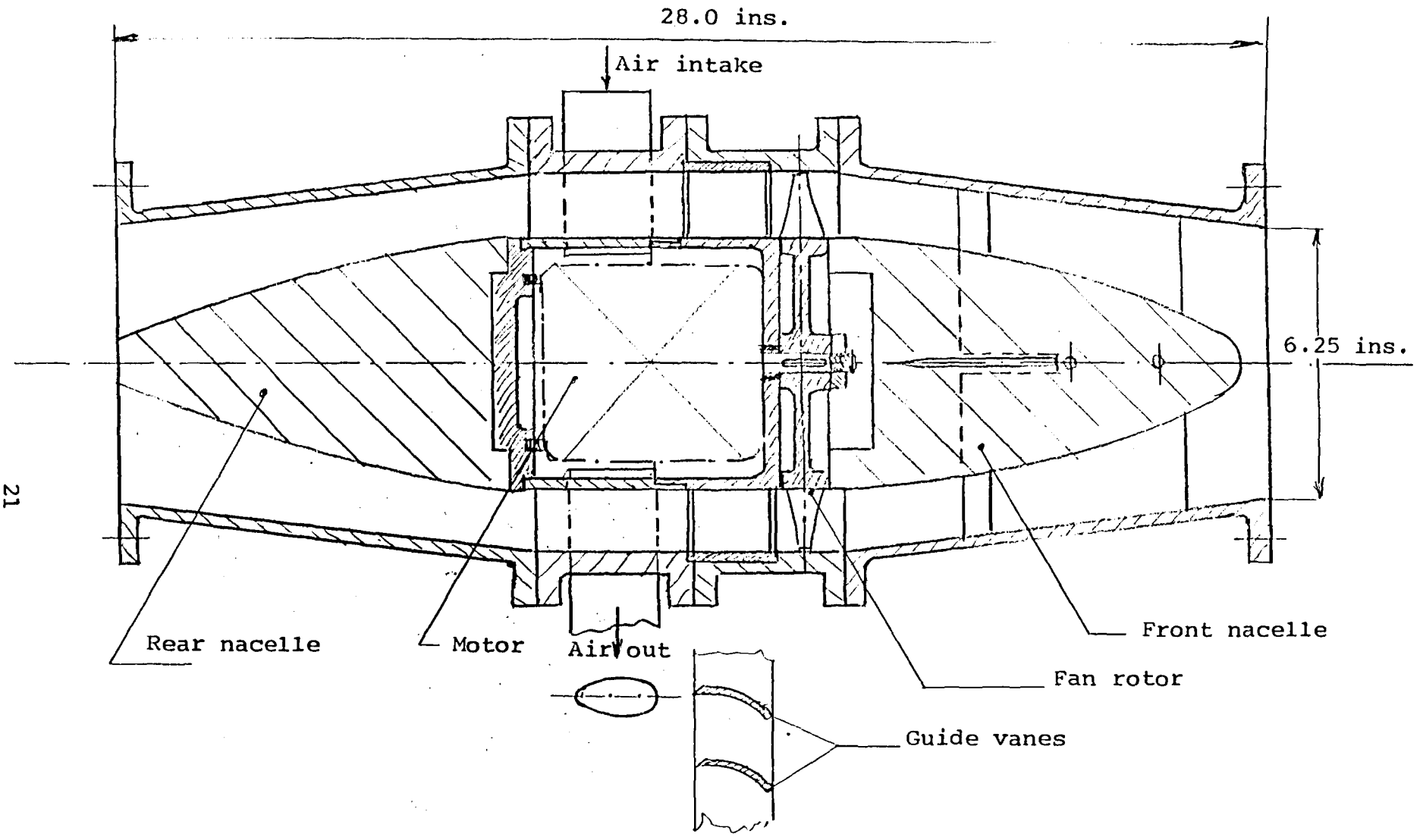

Figure 3/a. General arrangement of the fan section

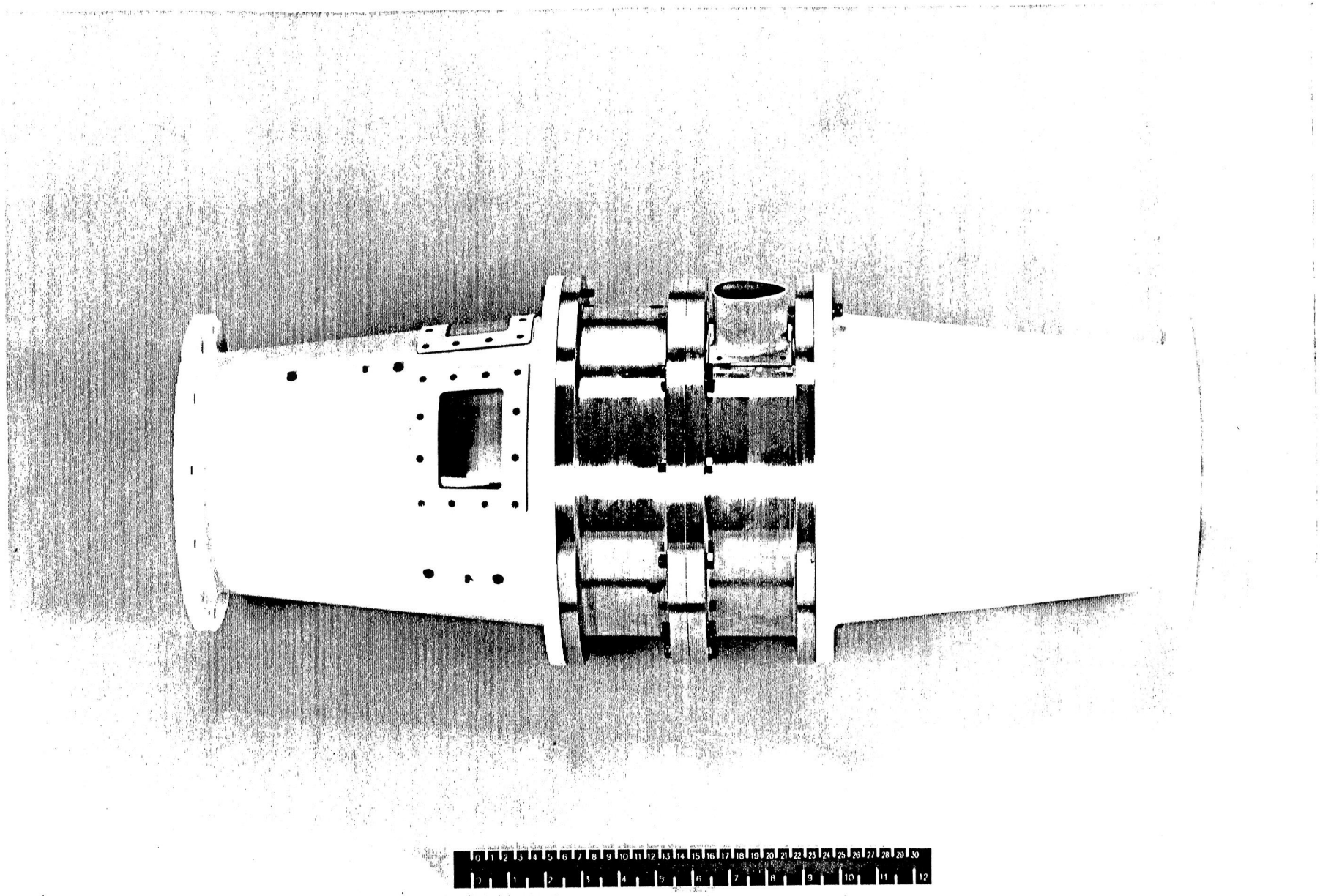

Figure 3/b. View of the fan section

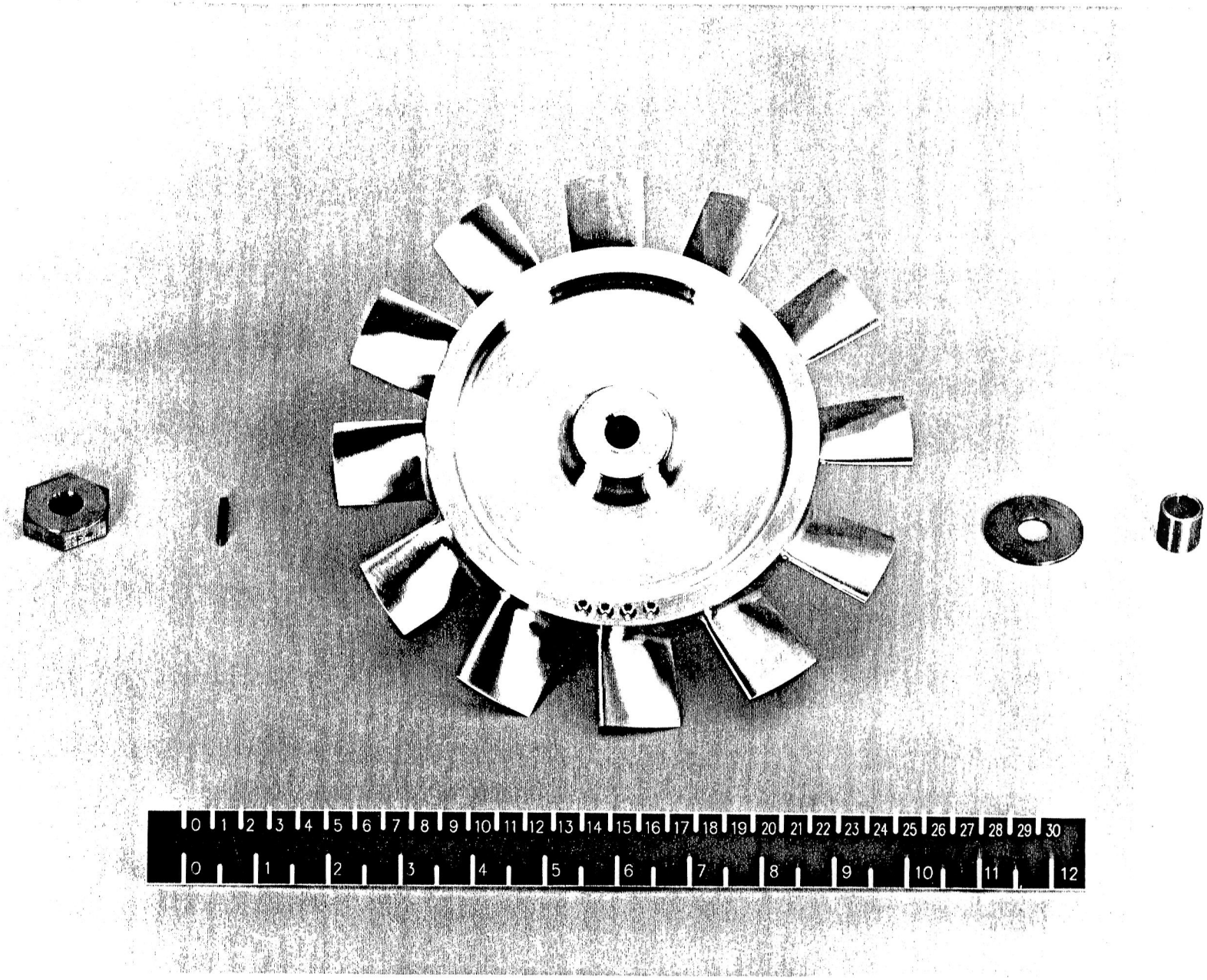

Figure 4. View of the axial flow fan

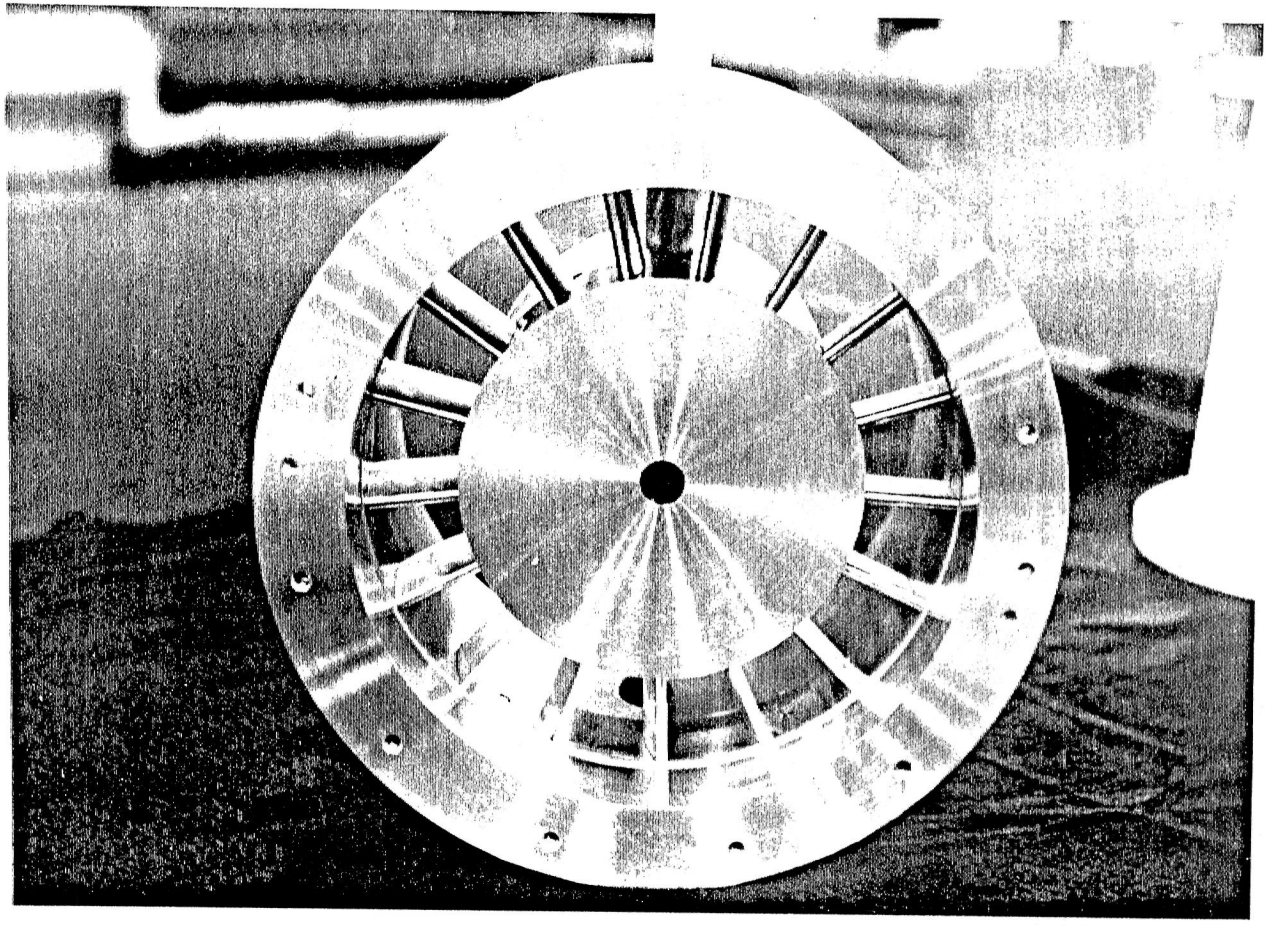

Figure 5. View of the guide vanes

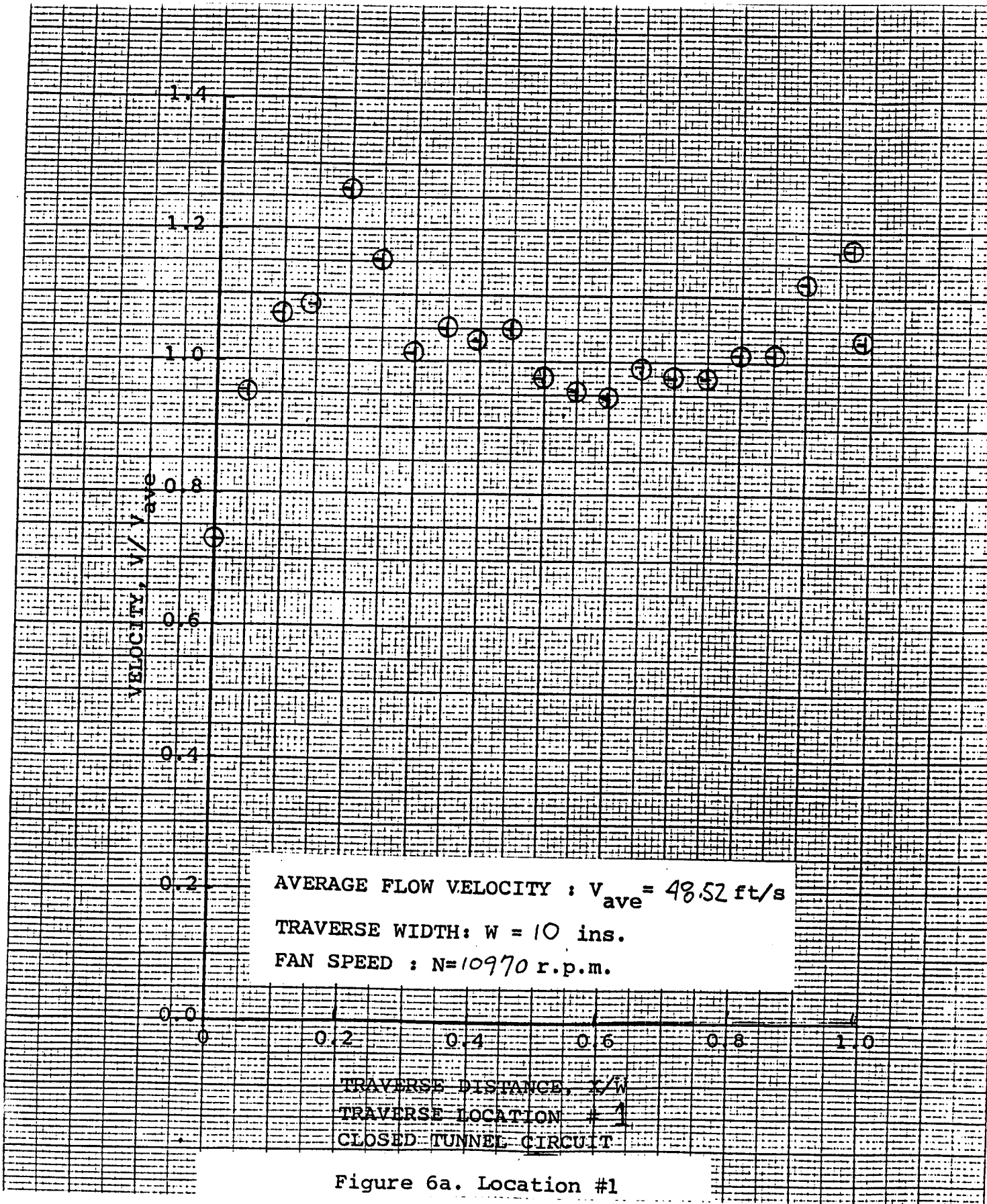

Figure 6a. Location #1

Figure 6. Horizontal velocity traverses with closed test section

CONTINUED

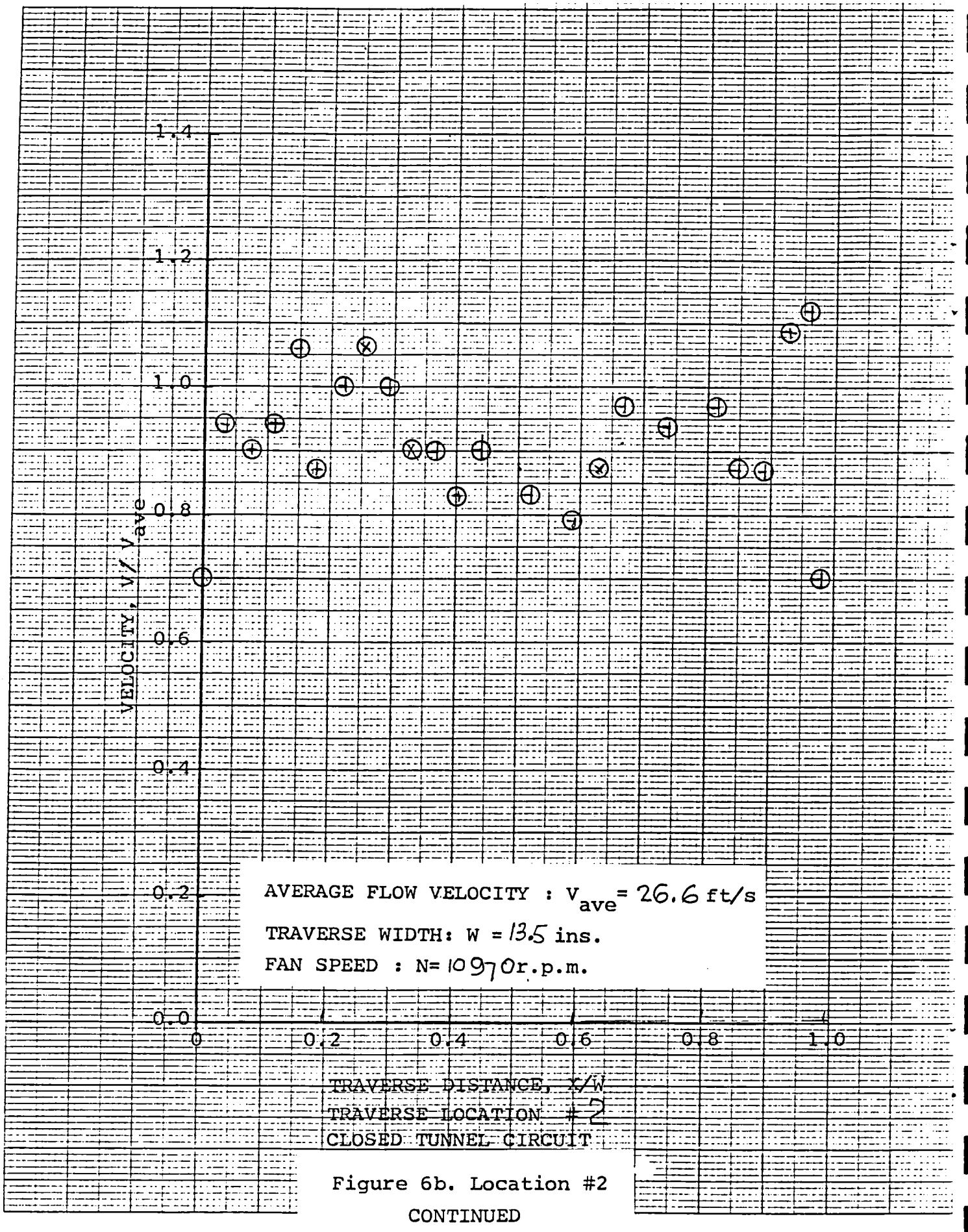

Figure 6b. Location #2
CONTINUED

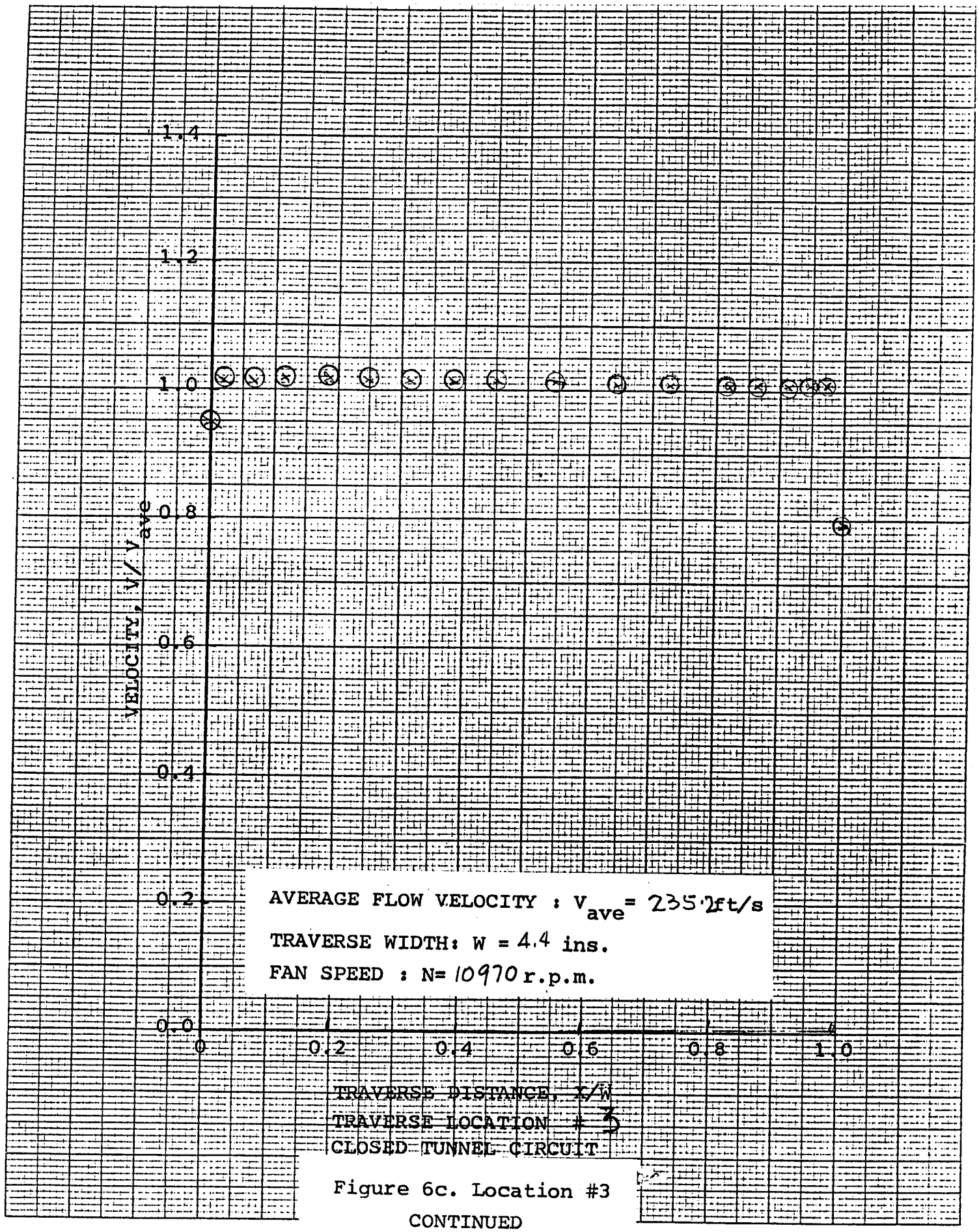

Figure 6c. Location #3

CONTINUED

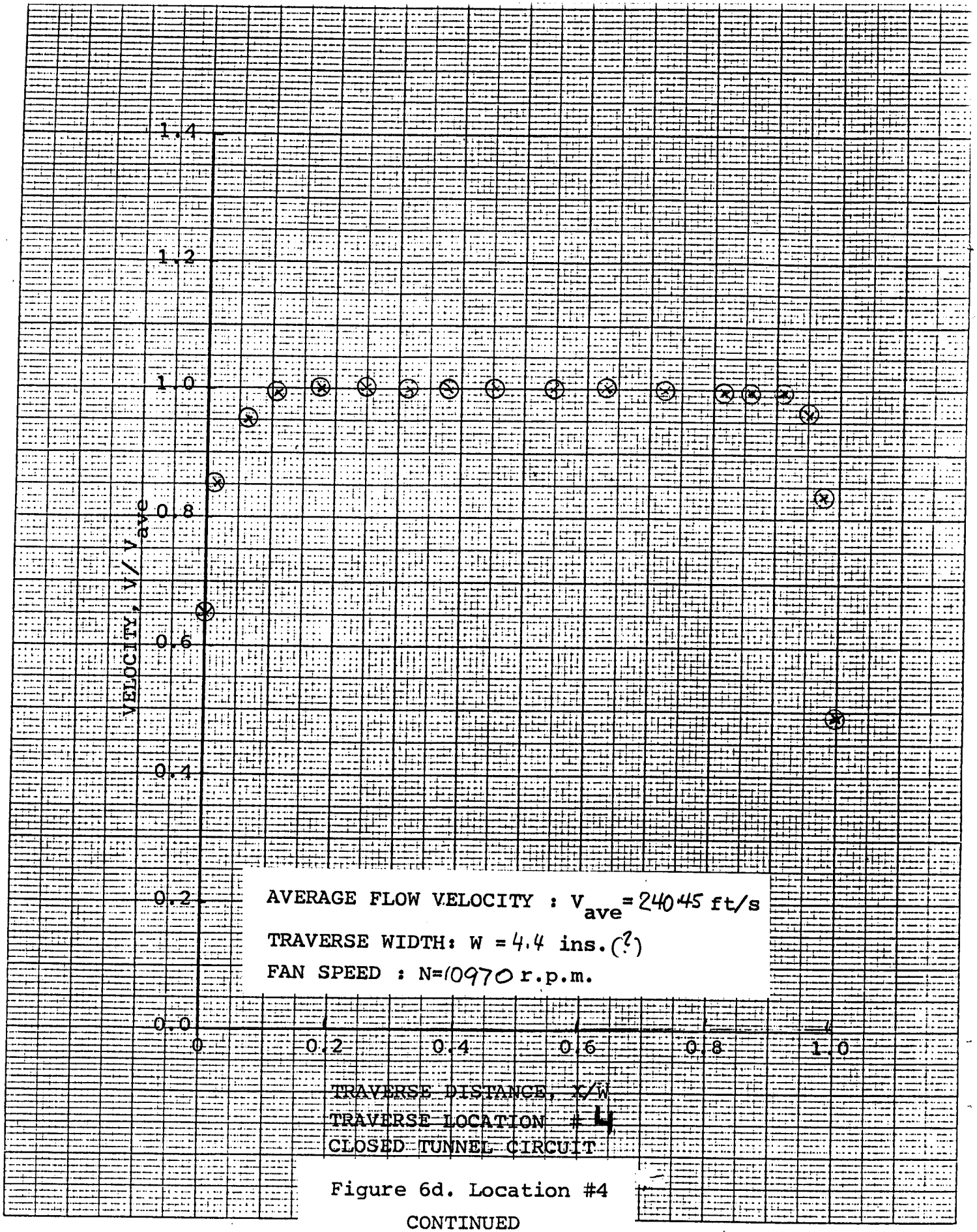

Figure 6d. Location #4

CONTINUED

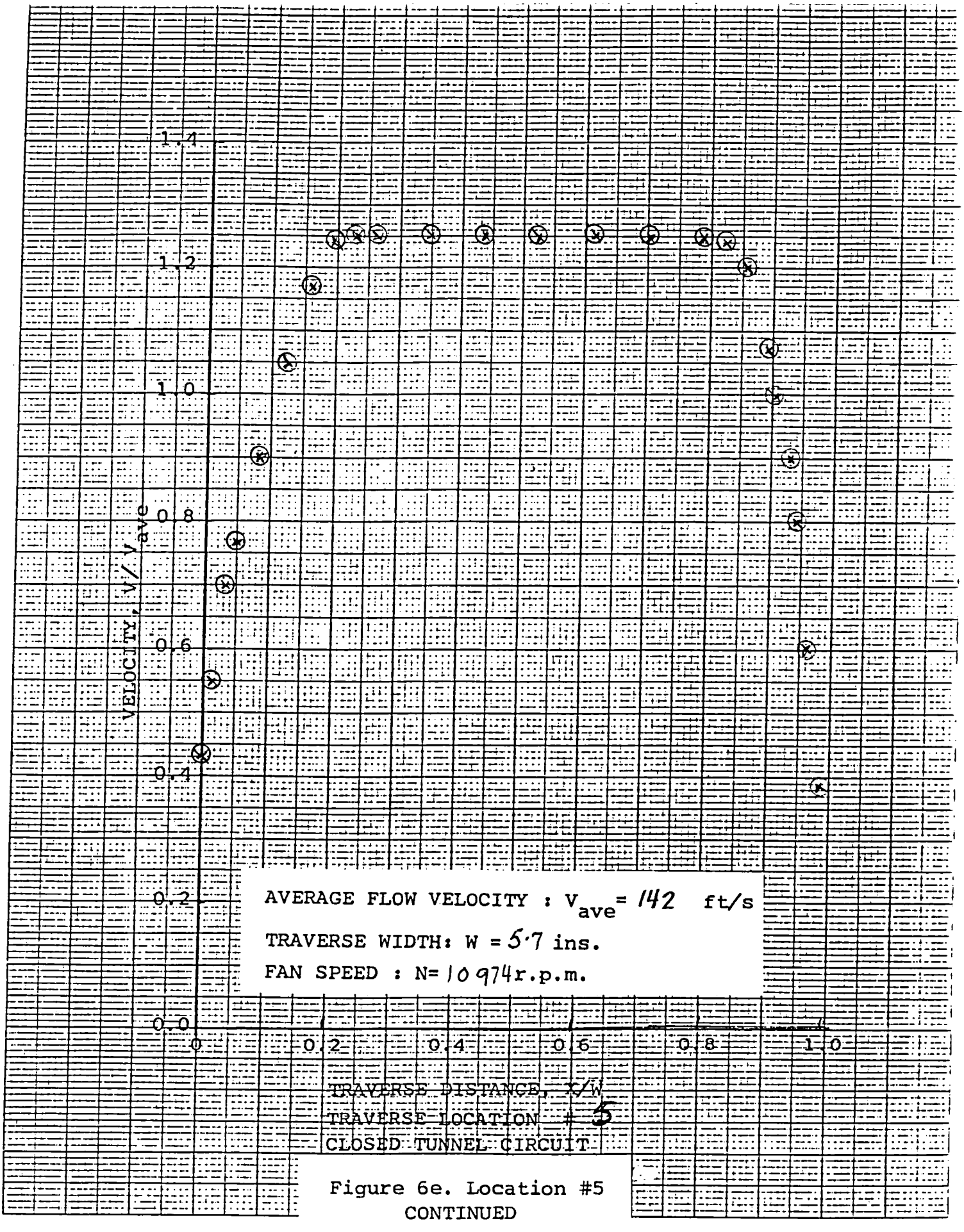

Figure 6e. Location #5
CONTINUED

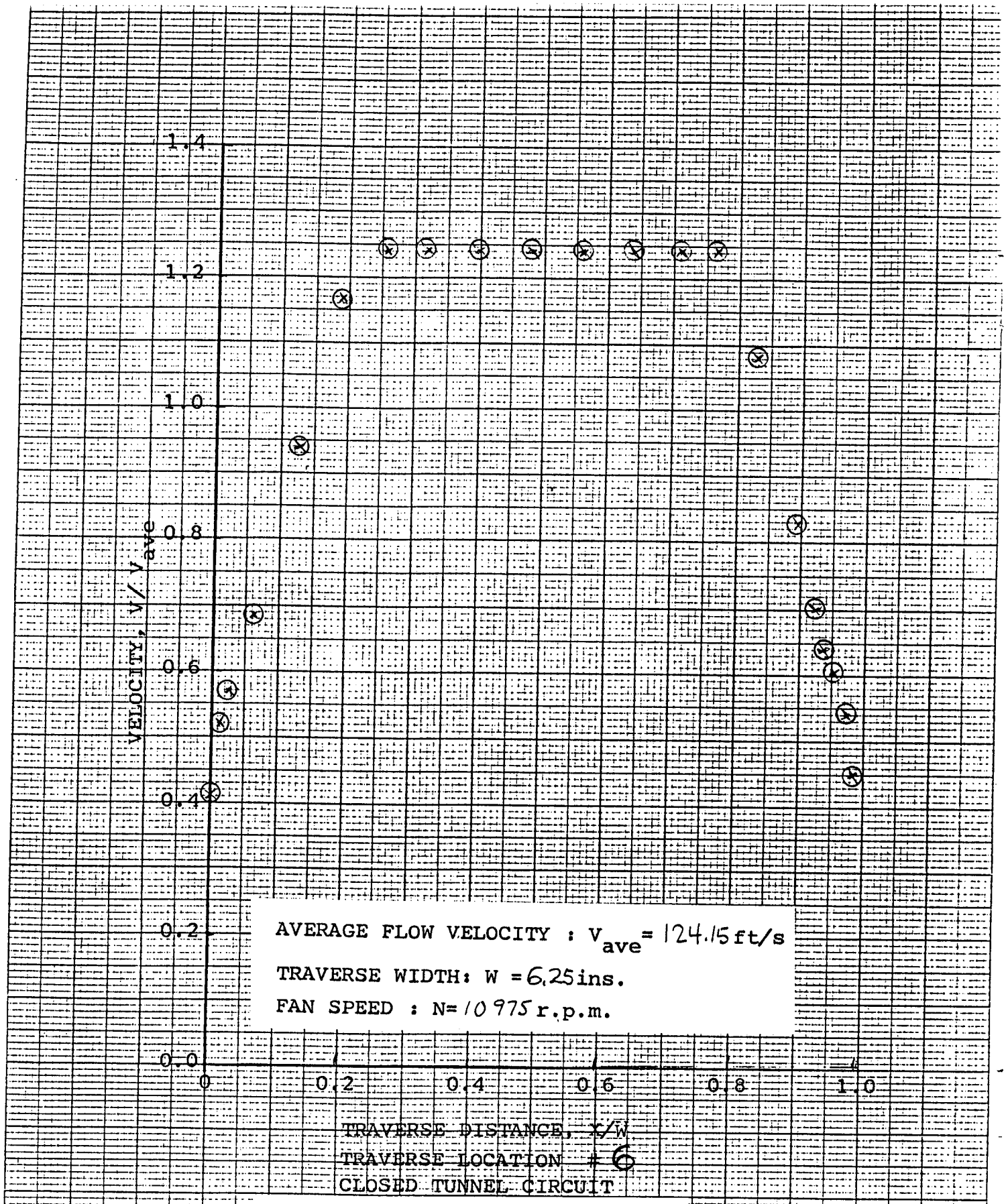

Figure 6f. Location #6
CONTINUED

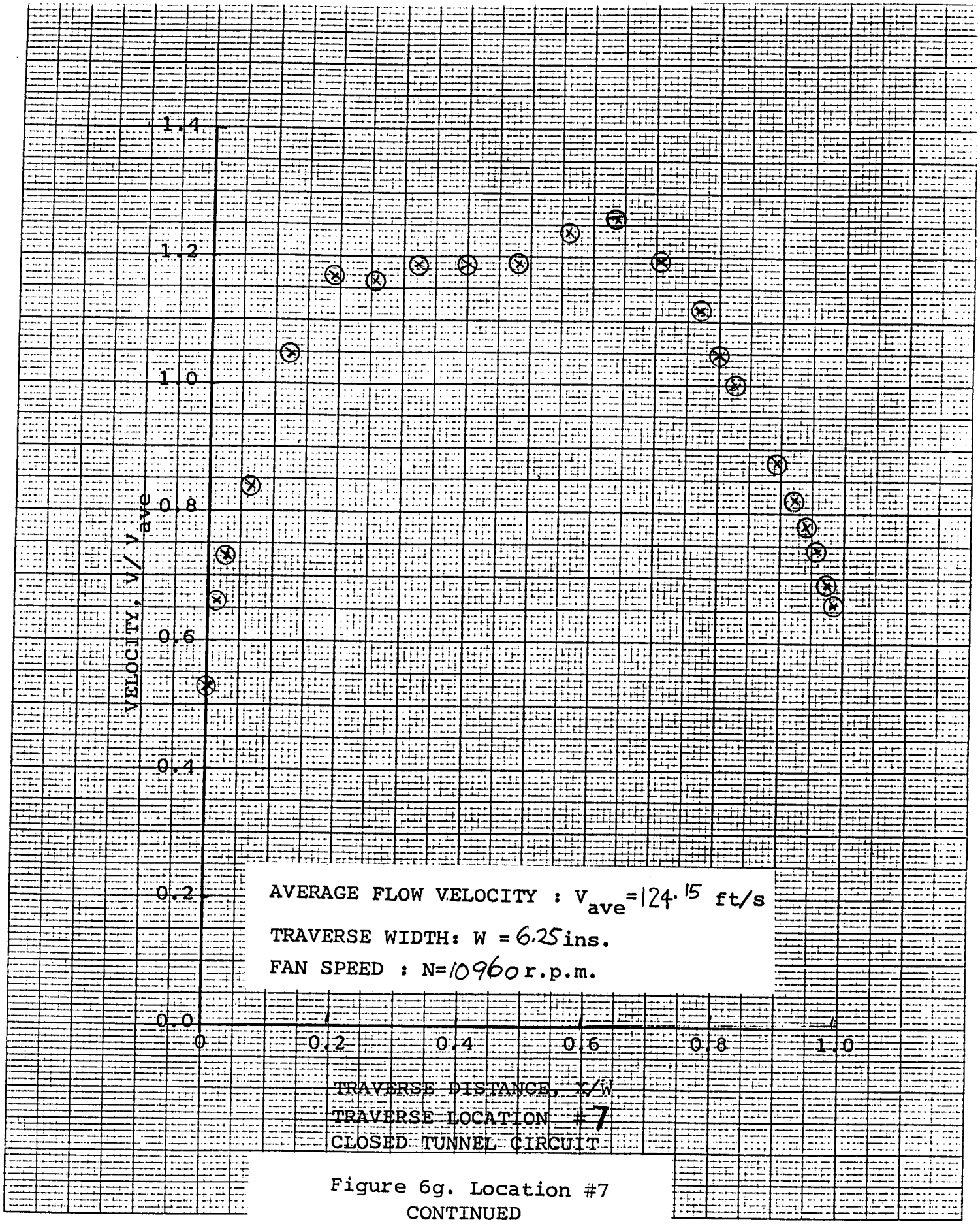

Figure 6g. Location #7
CONTINUED

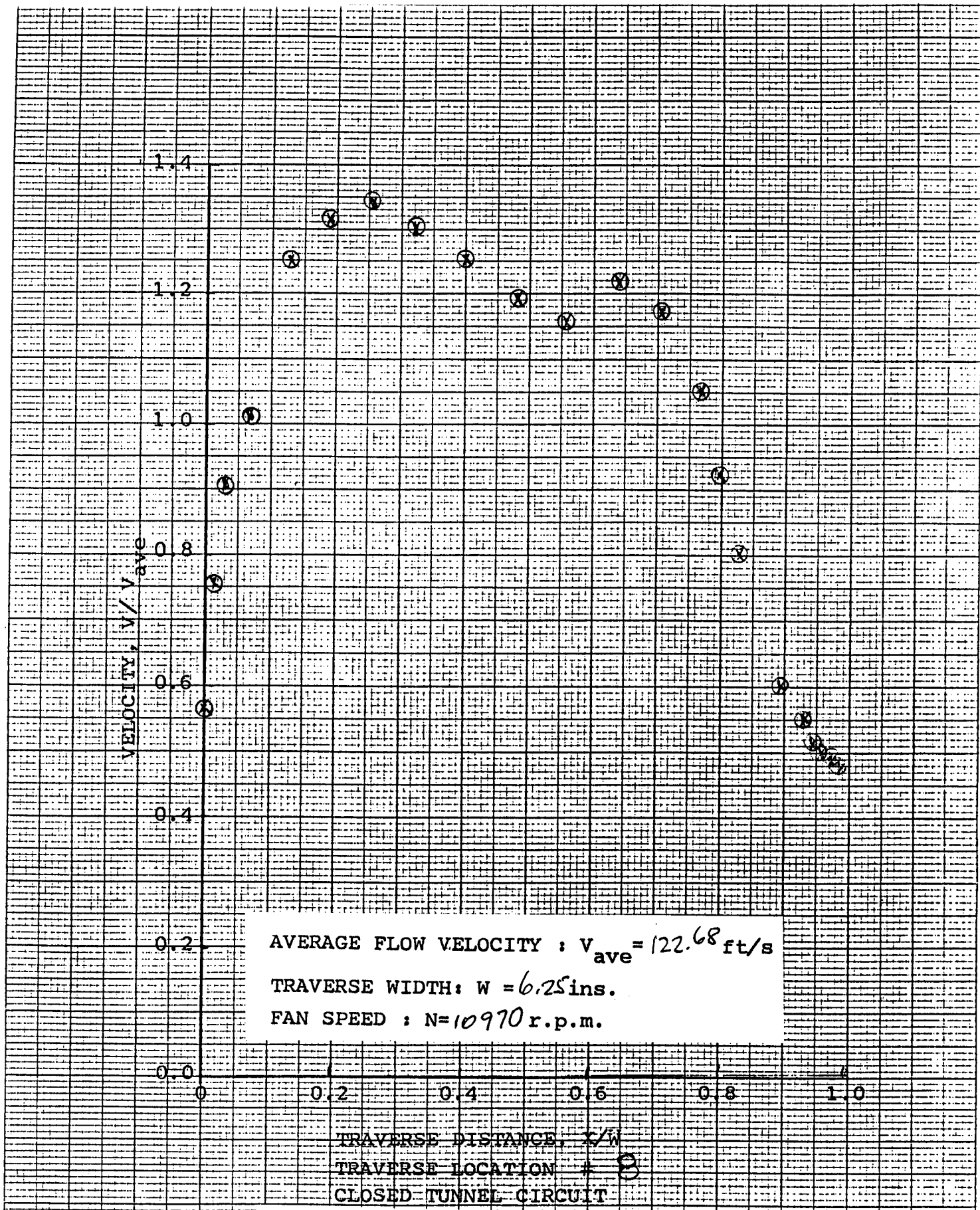

Figure 6h. Location #8

CONTINUED

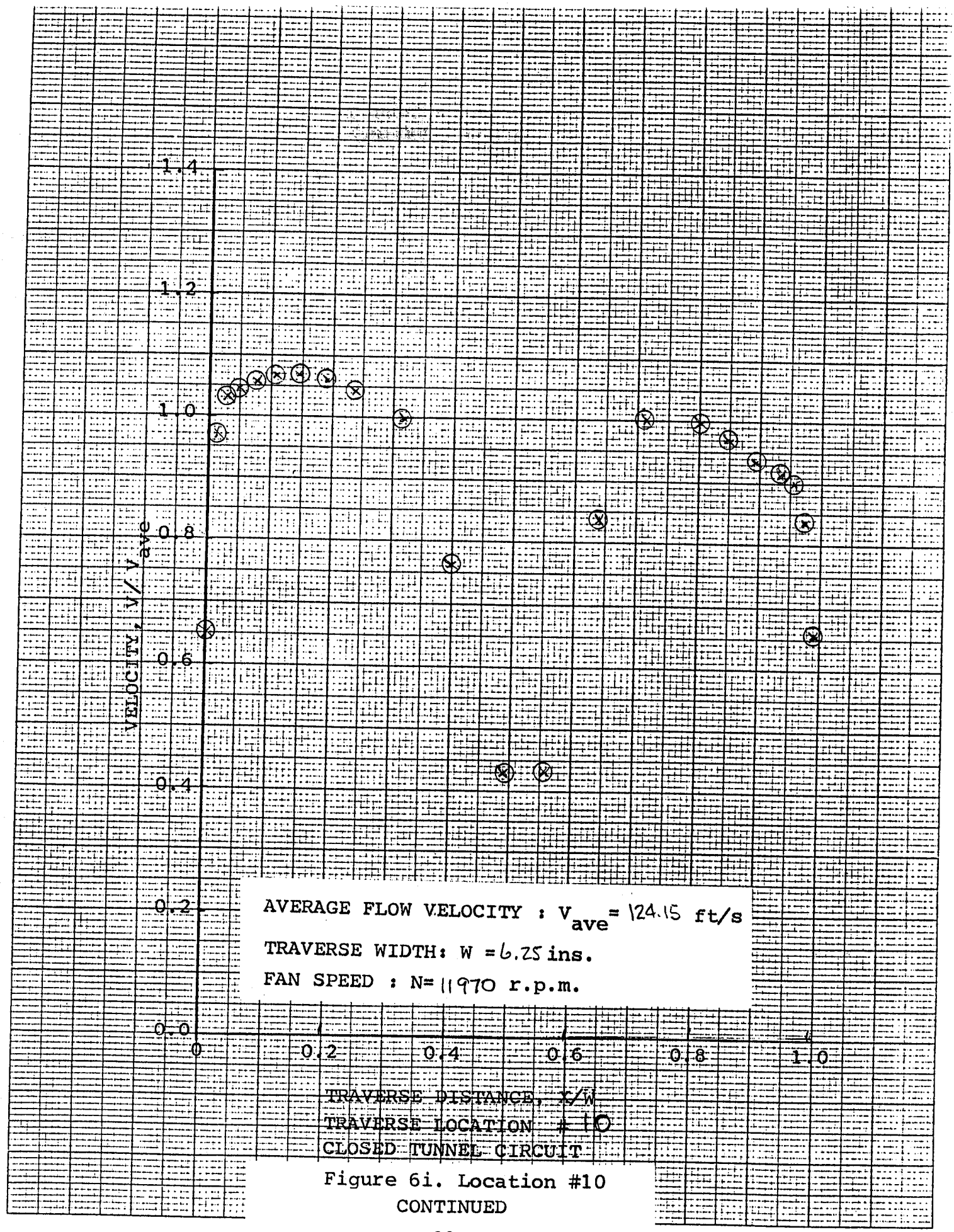

Figure 6i. Location #10
CONTINUED

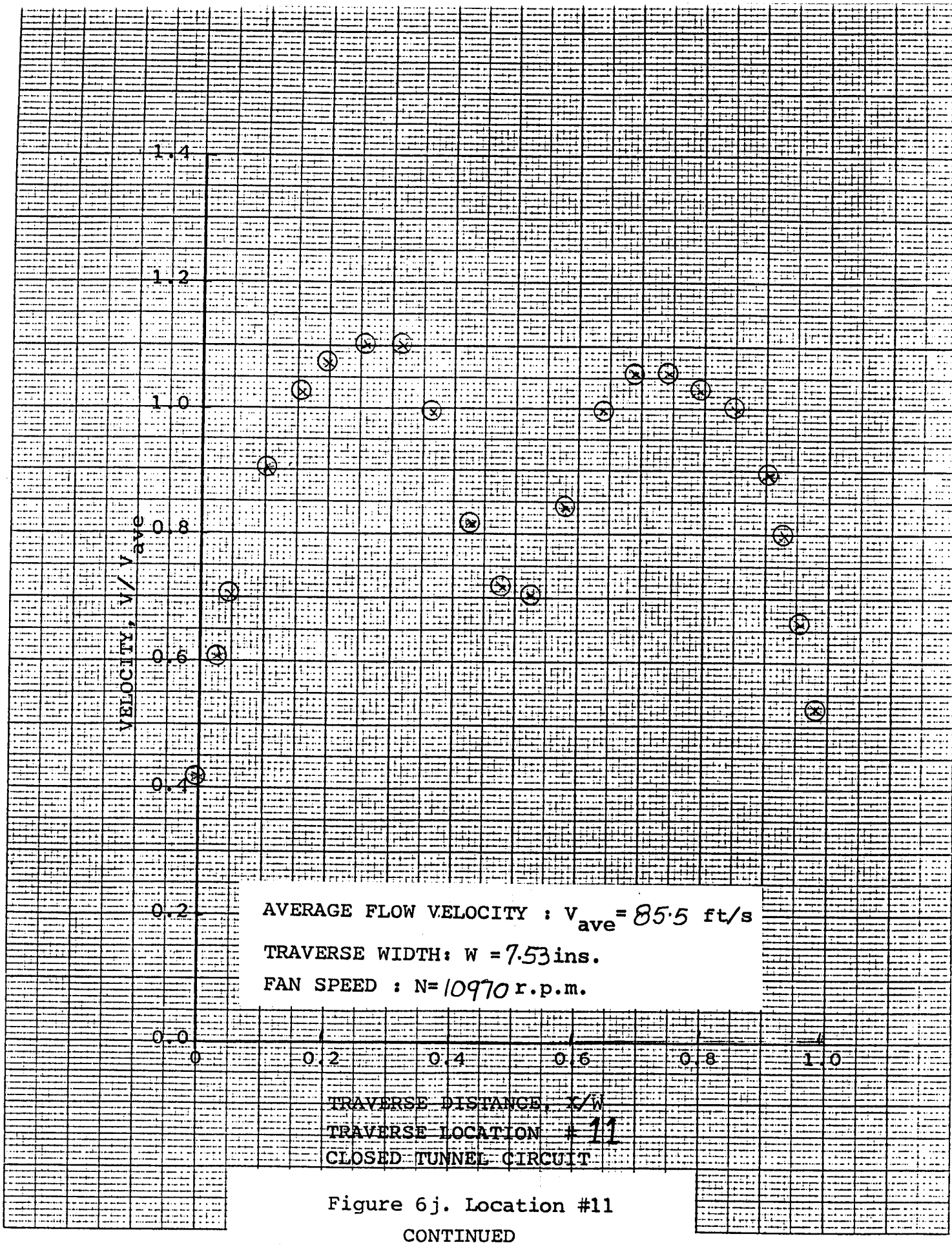

Figure 6j. Location #11
CONTINUED

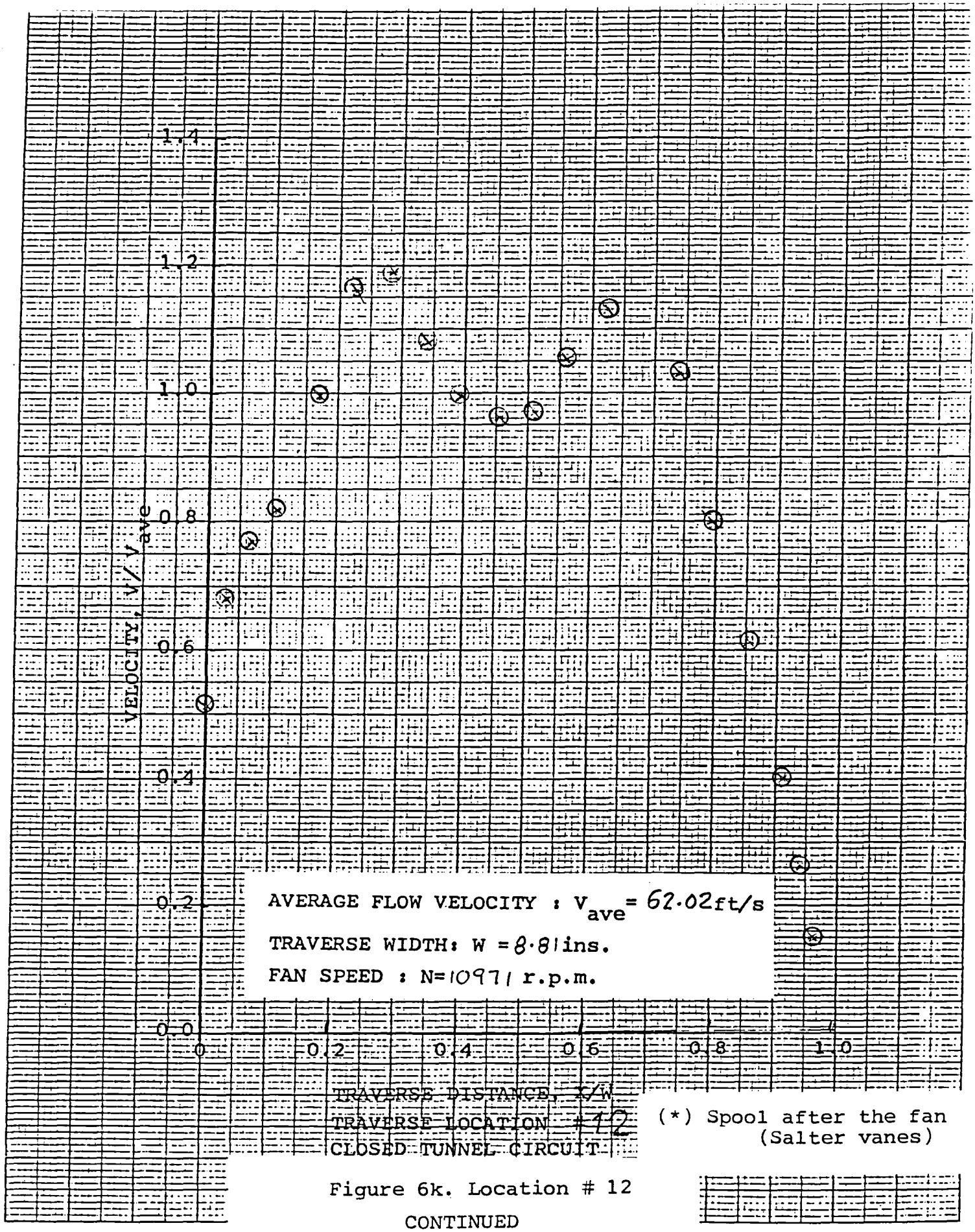

(*) Spool after the fan (Salter vanes)

Figure 6k. Location # 12

CONTINUED

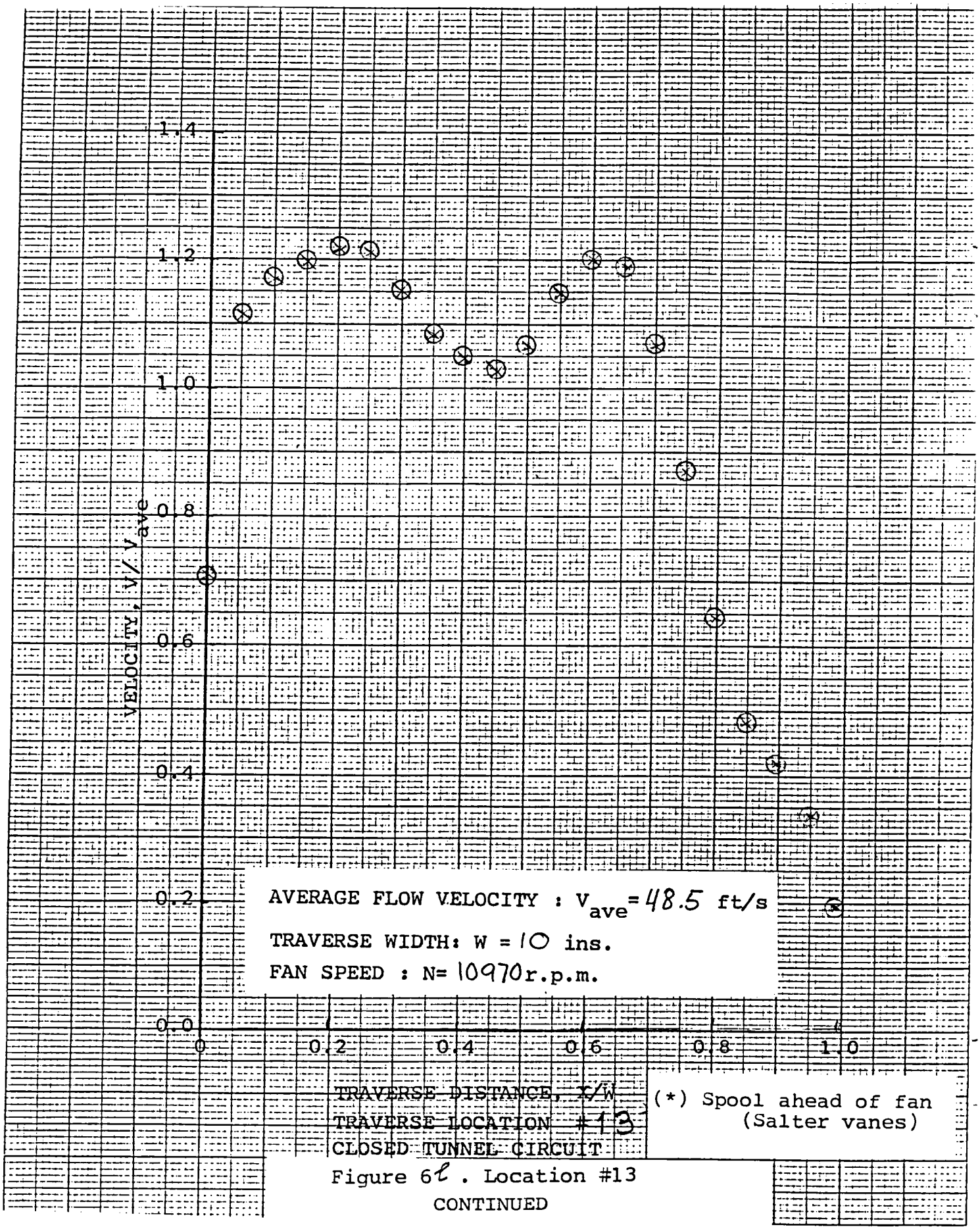

Figure 6ℓ . Location #13
CONTINUED

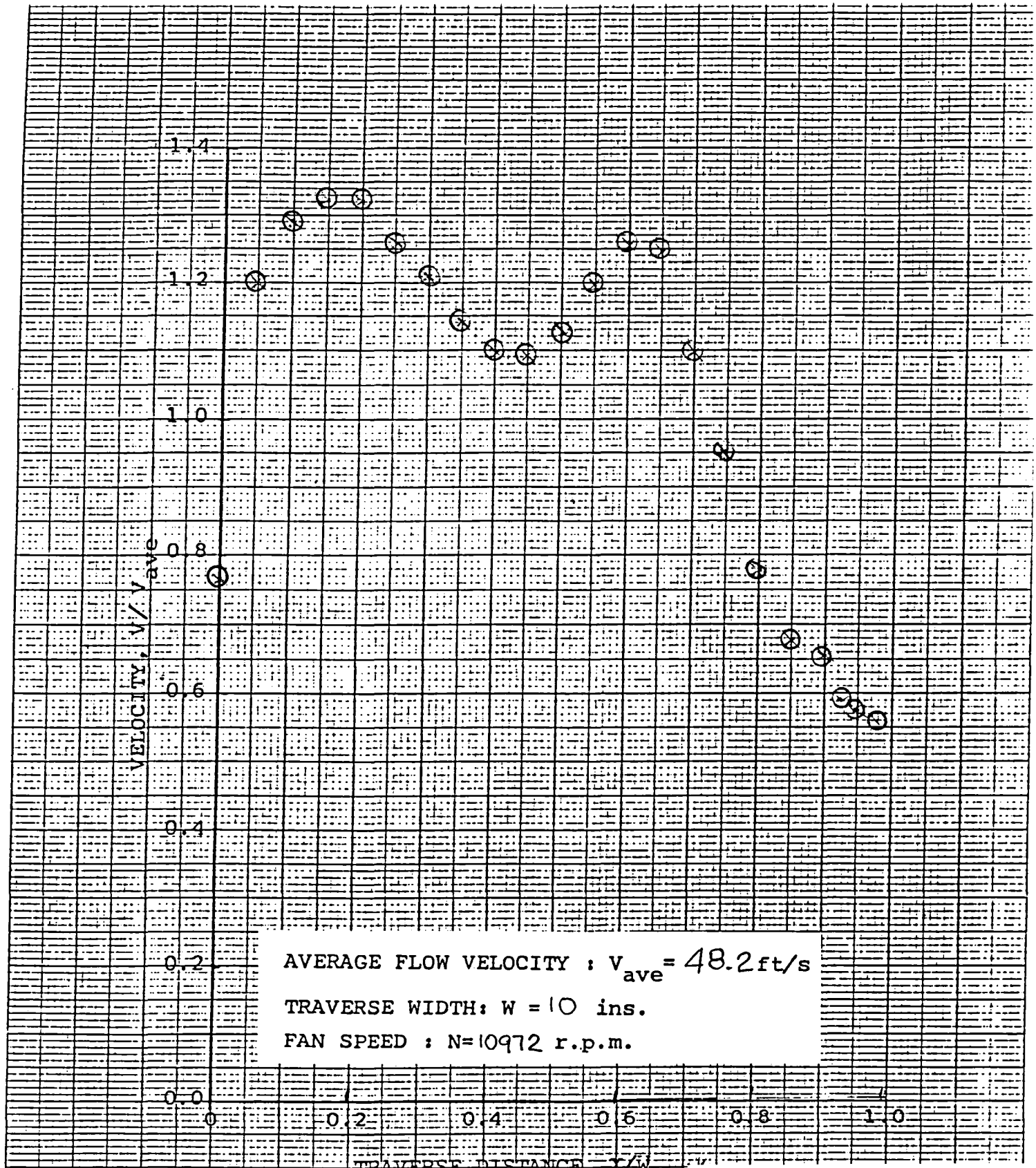

AVERAGE FLOW VELOCITY : V_{ave} = 48.2 ft/s

TRAVERSE WIDTH: W = 10 ins.

FAN SPEED : N= 10972 r.p.m.

TRAVERSE LOCATION # 13

(*) Spool after the fan (Salter vanes)

CLOSED TUNNEL CIRCUIT

Figure 6m. Location #13 (same as 6ℓ)

CONTINUED

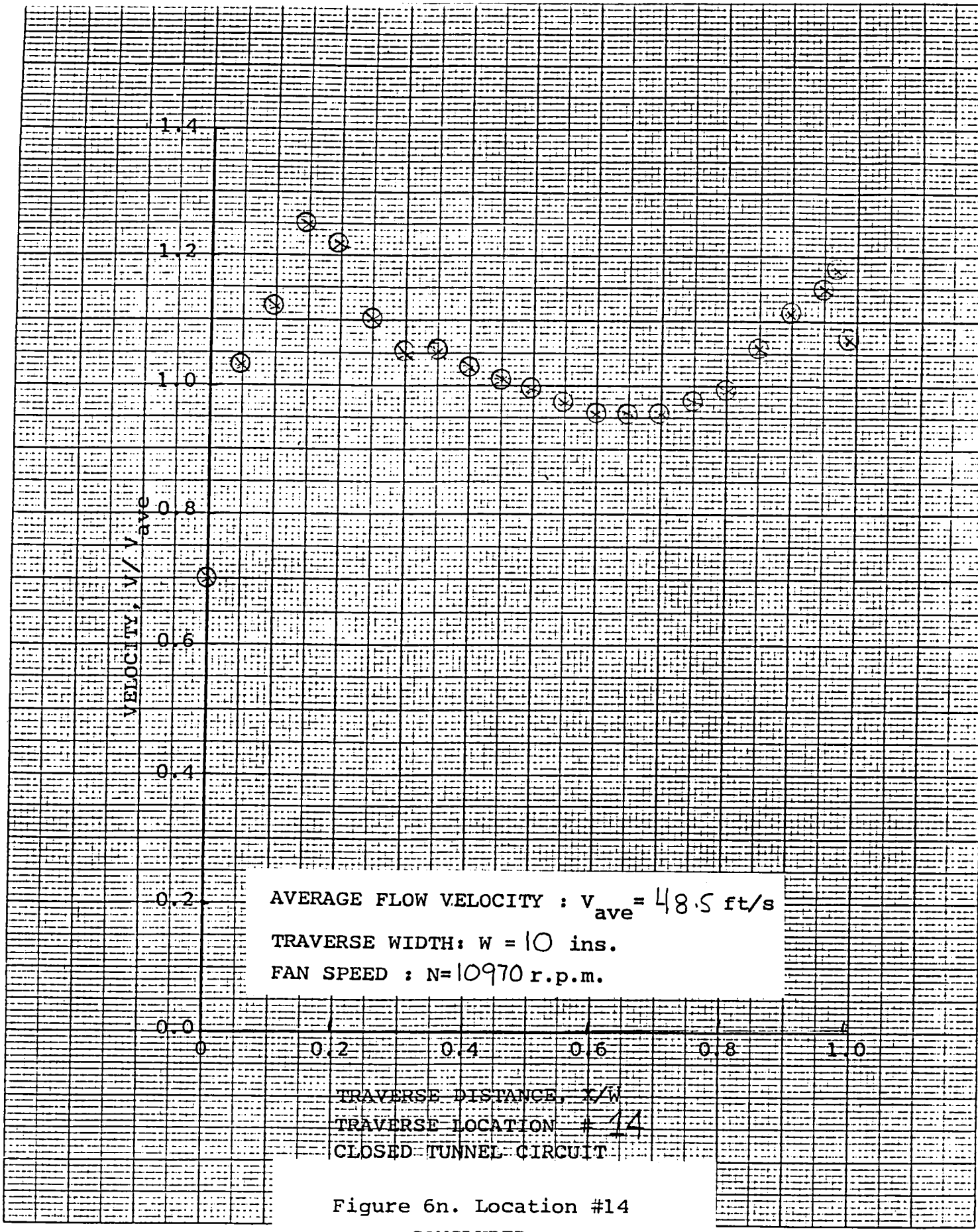

Figure 6n. Location #14
CONCLUDED

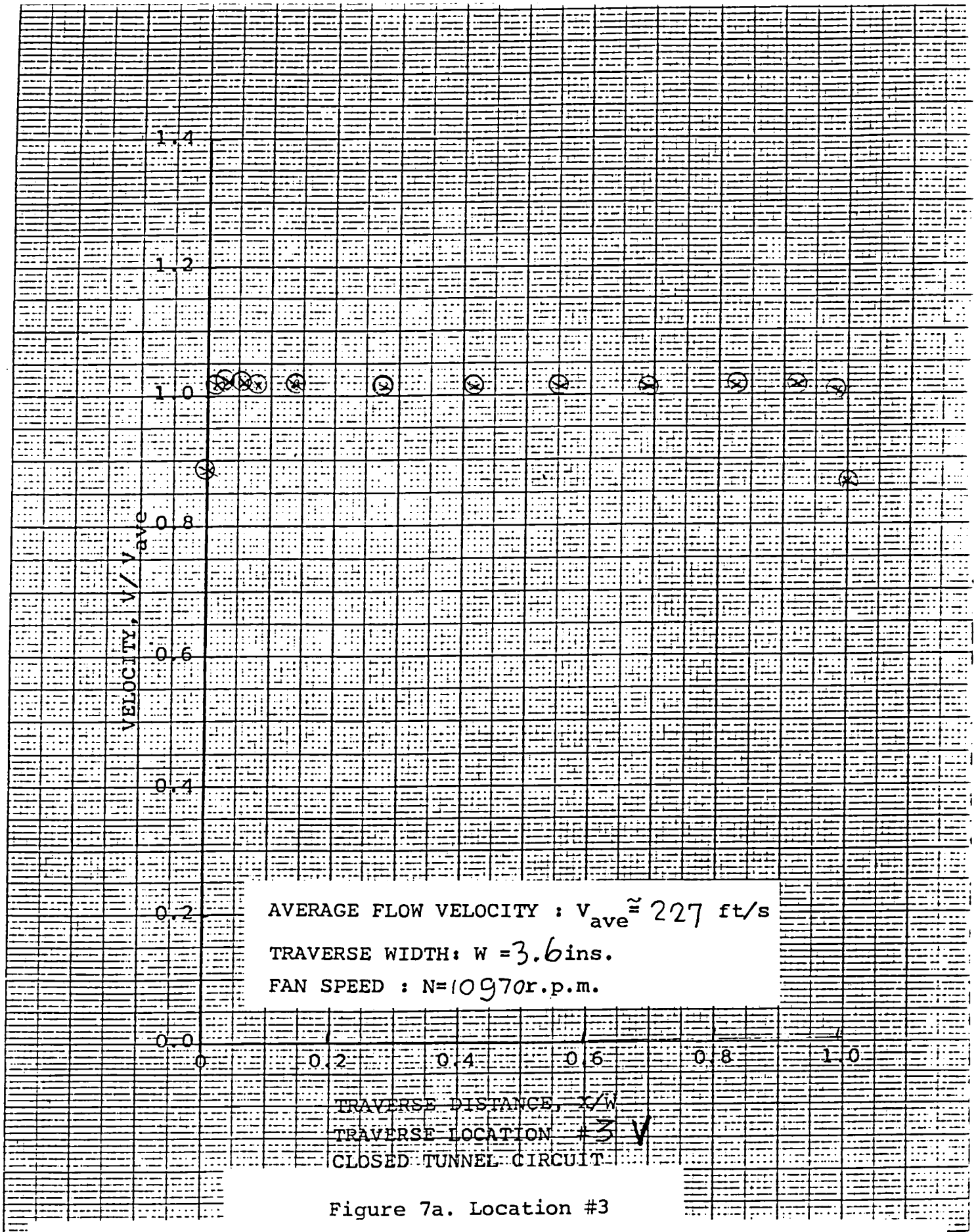

Figure 7a. Location #3

Figure 7. Vertical velocity traverses with closed test section

CONTINUED

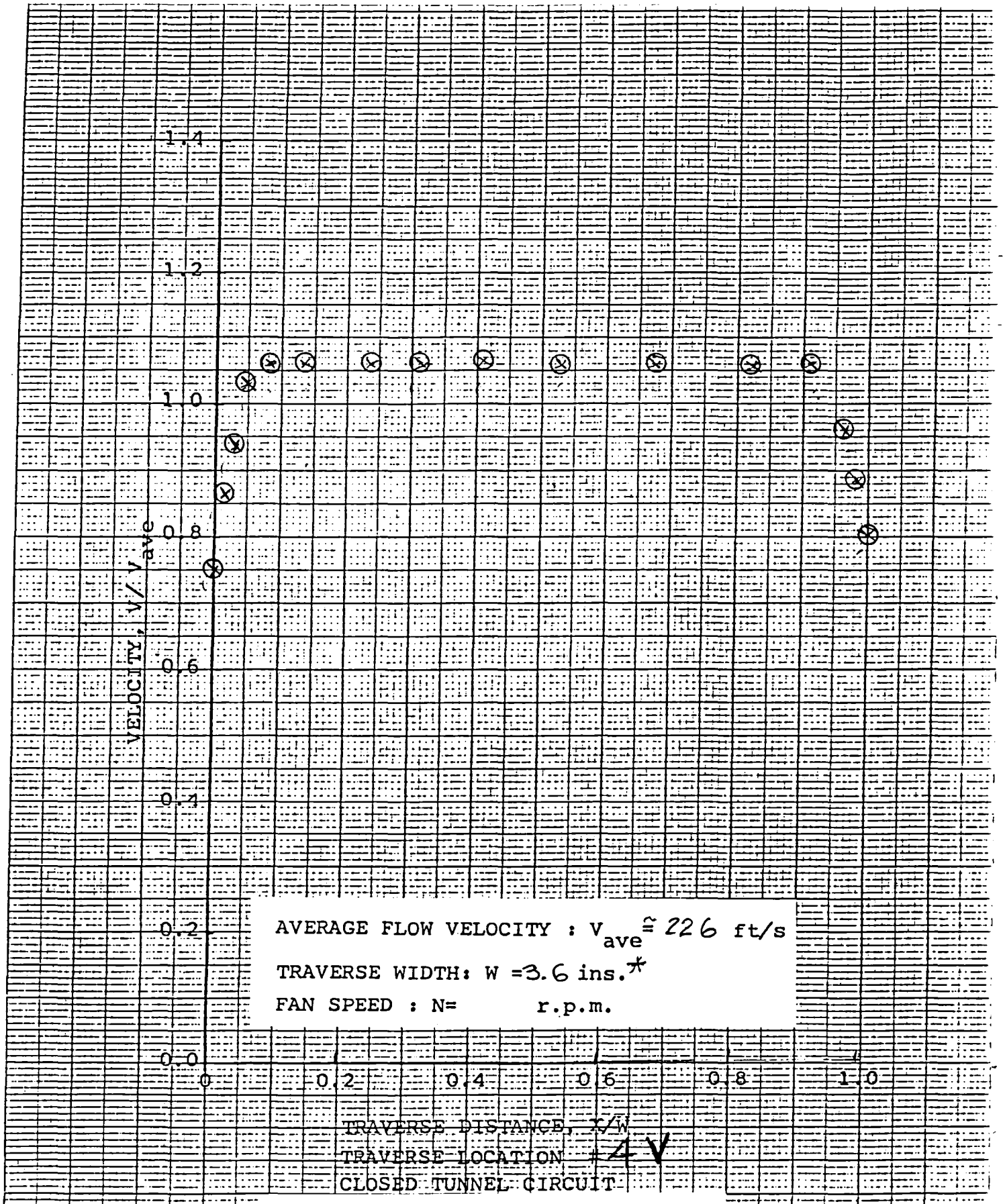

Figure 7b. Location #4

CONTINUED

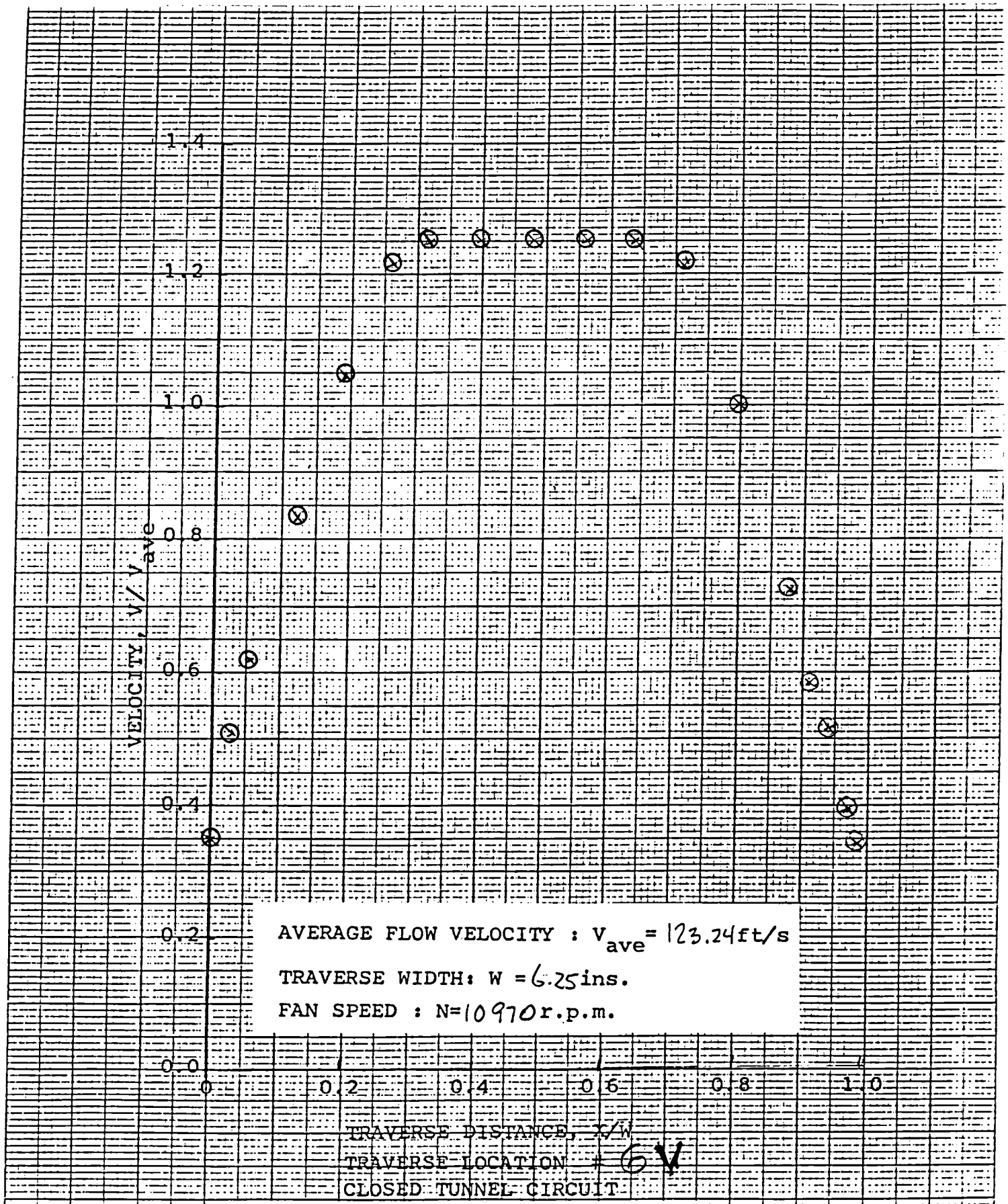

Figure 7c. Location #6
CONCLUDED

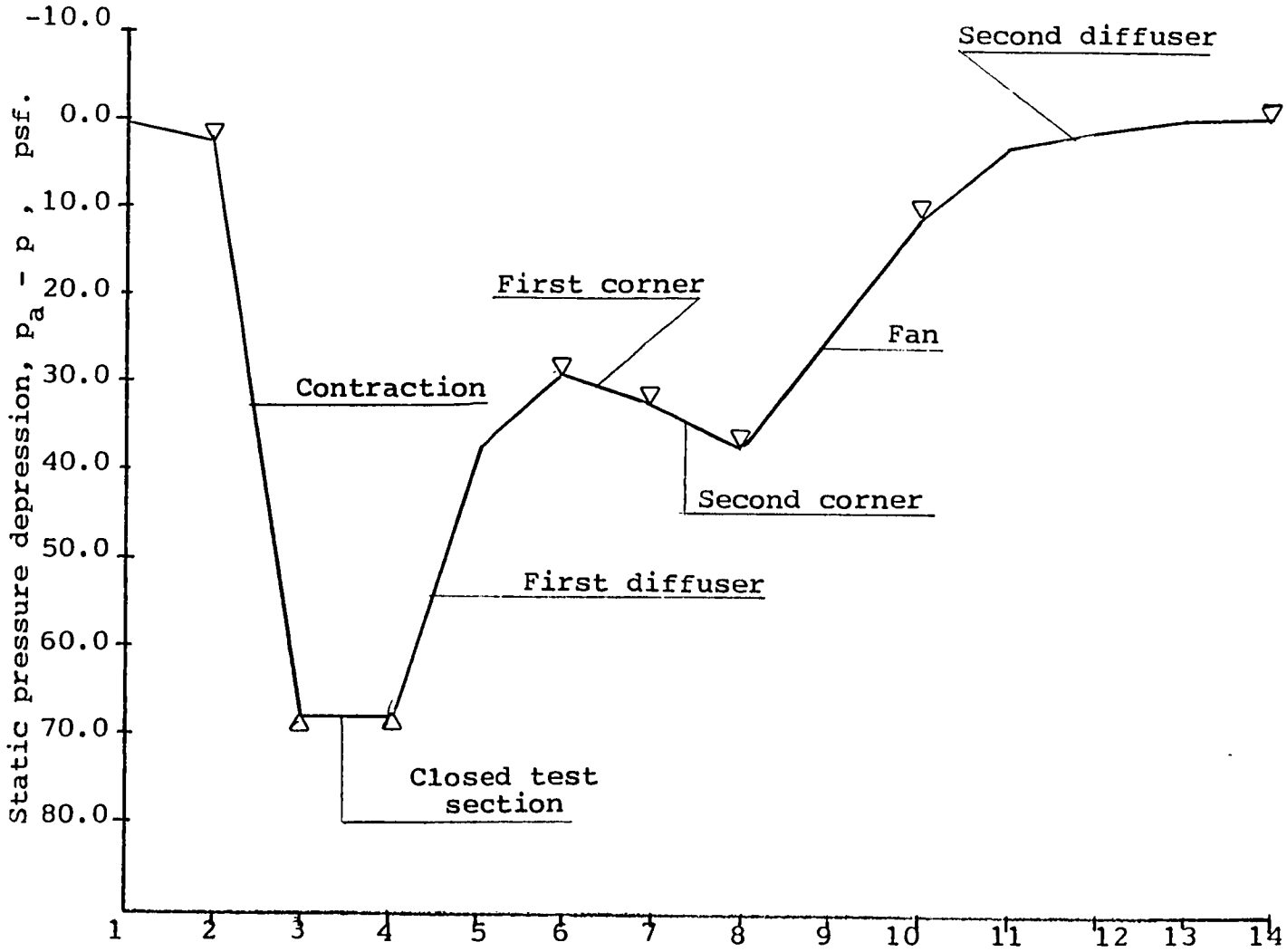

Figure 8. Pressure distribution around the the circuit with the closed test section

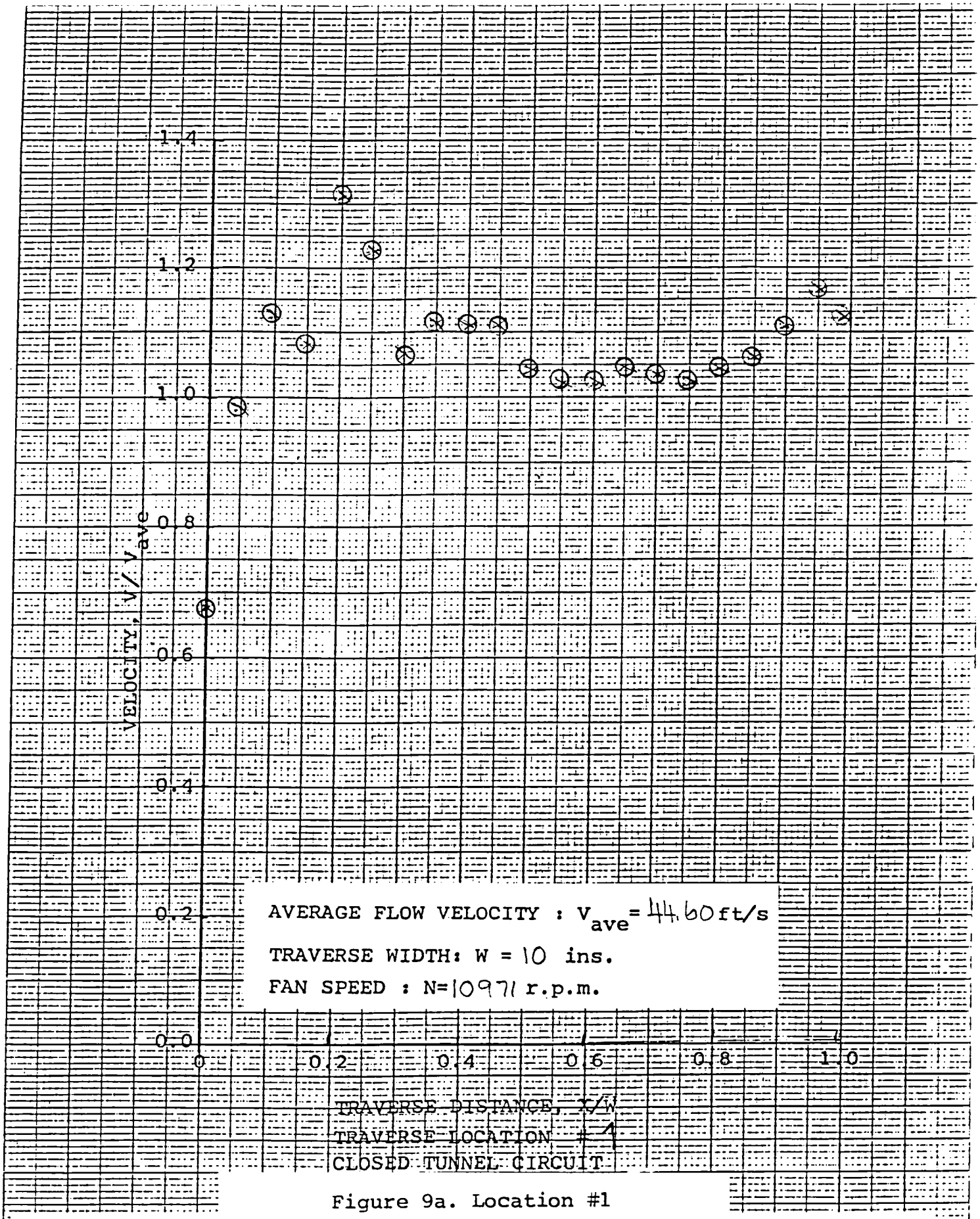

Figure 9a. Location #1

Figure 9. Horizontal velocity traverses with open test section
CONTINUED

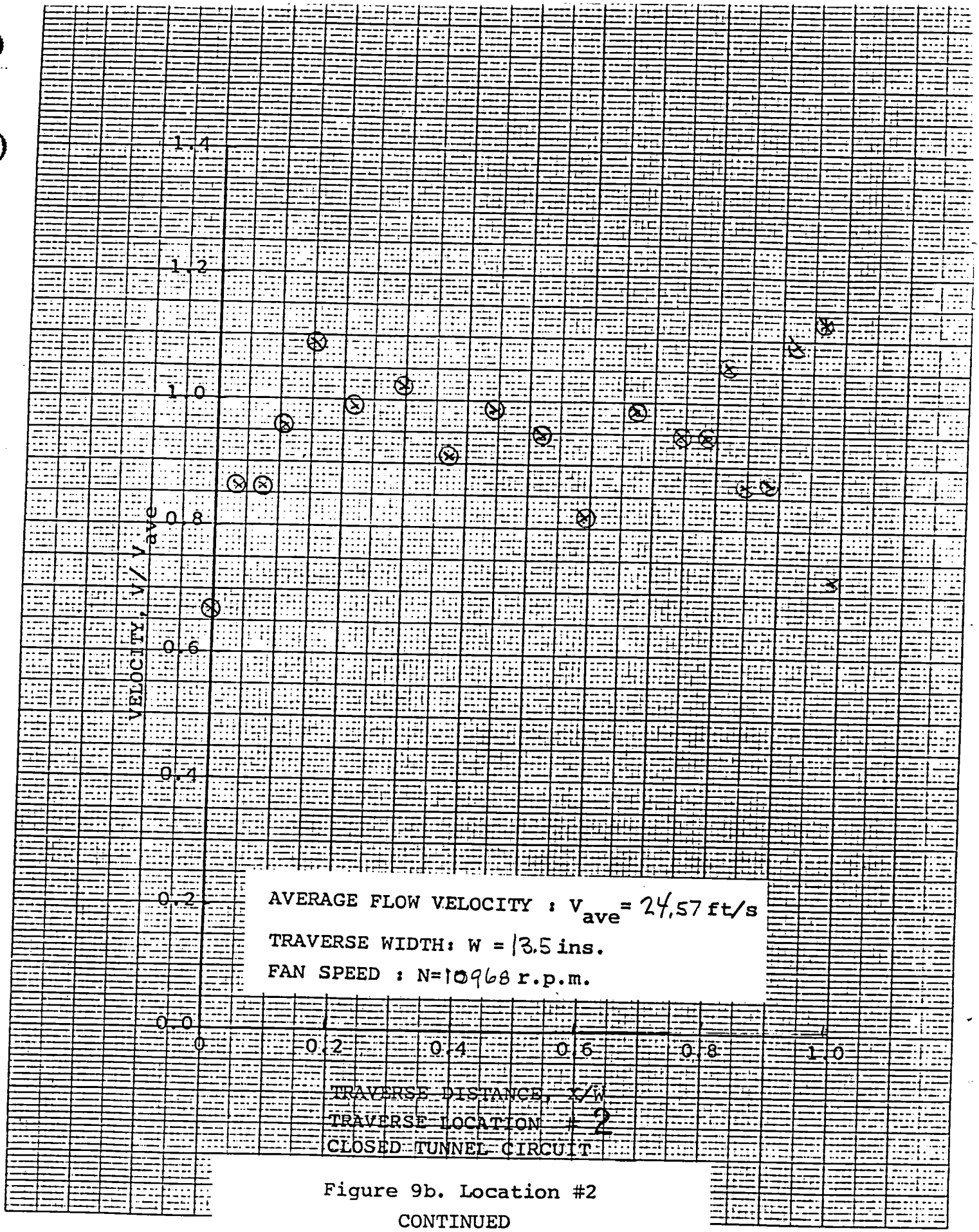

Figure 9b. Location #2
CONTINUED

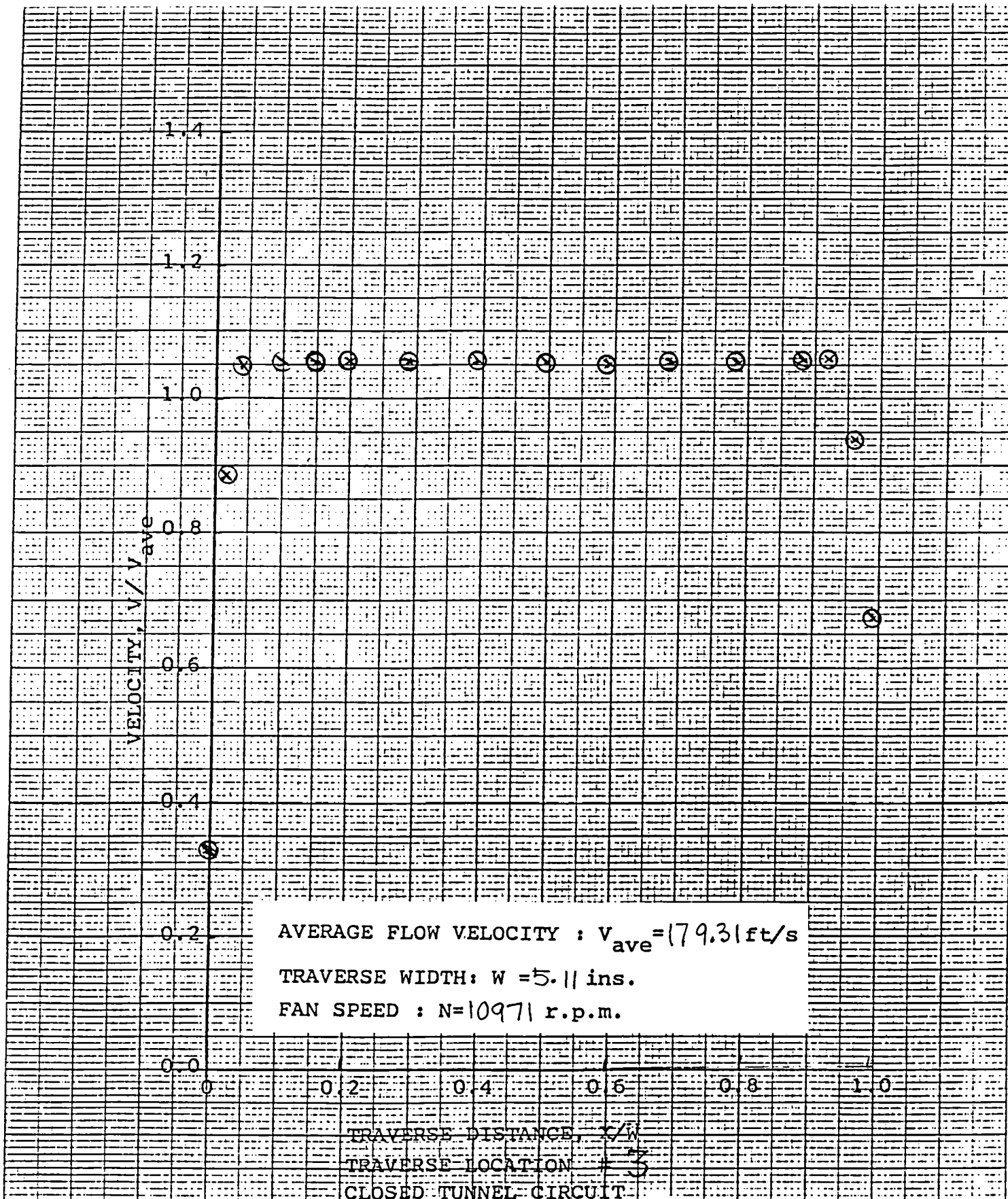

Figure 9c. Location #3
CONTINUED

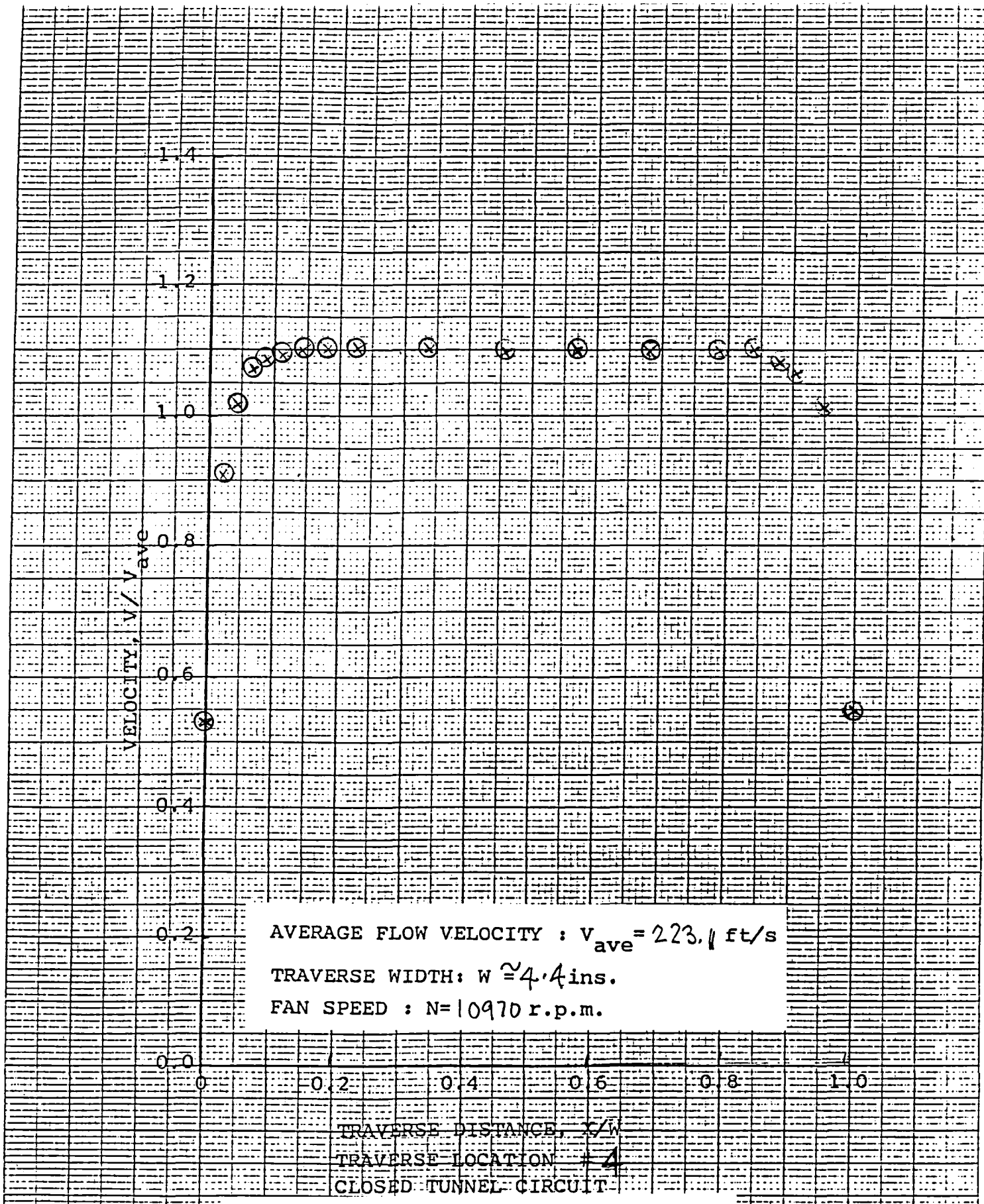

Figure 9d. Location #4
CONTINUED

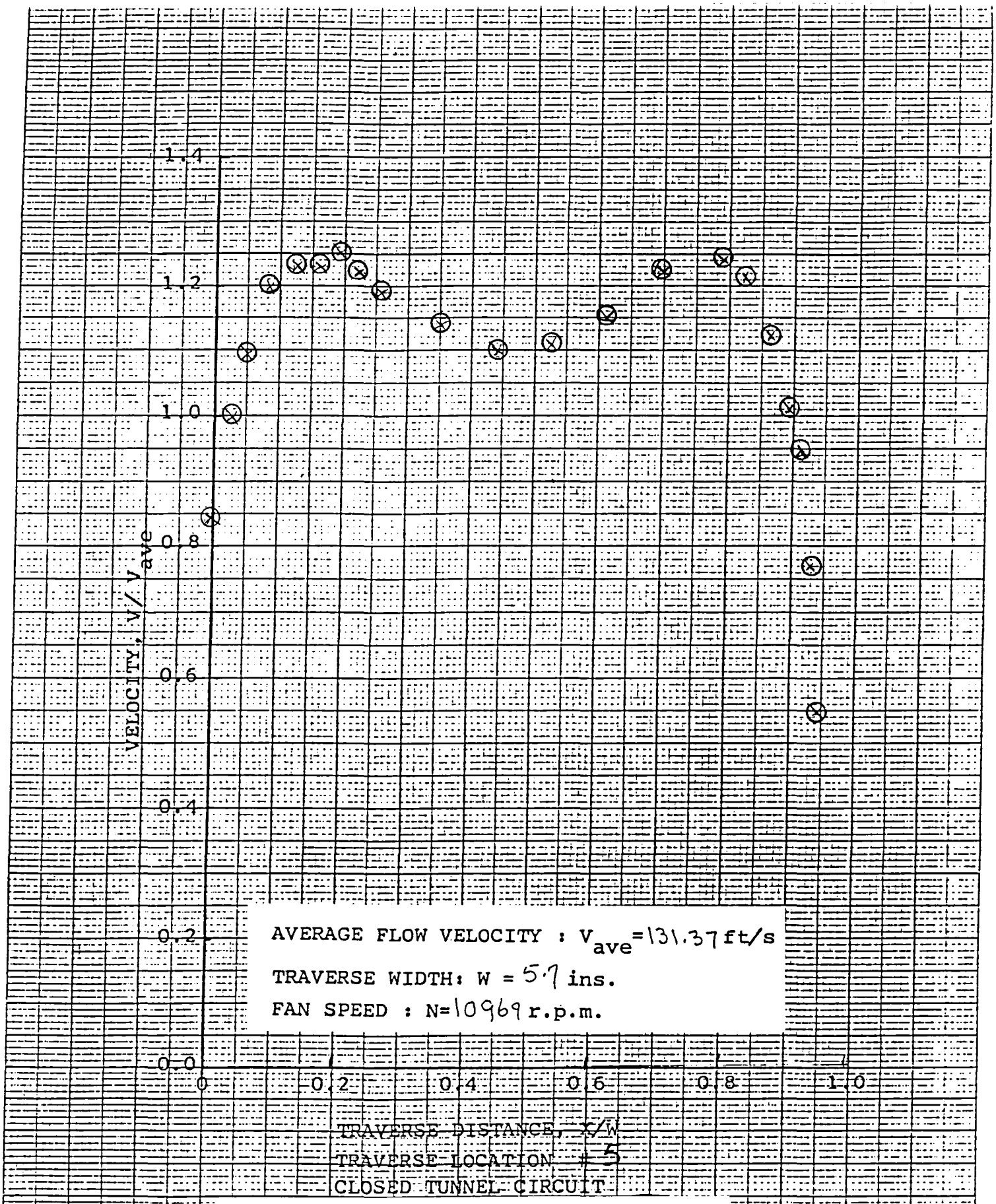

Figure 9e. Location #5
CONTINUED

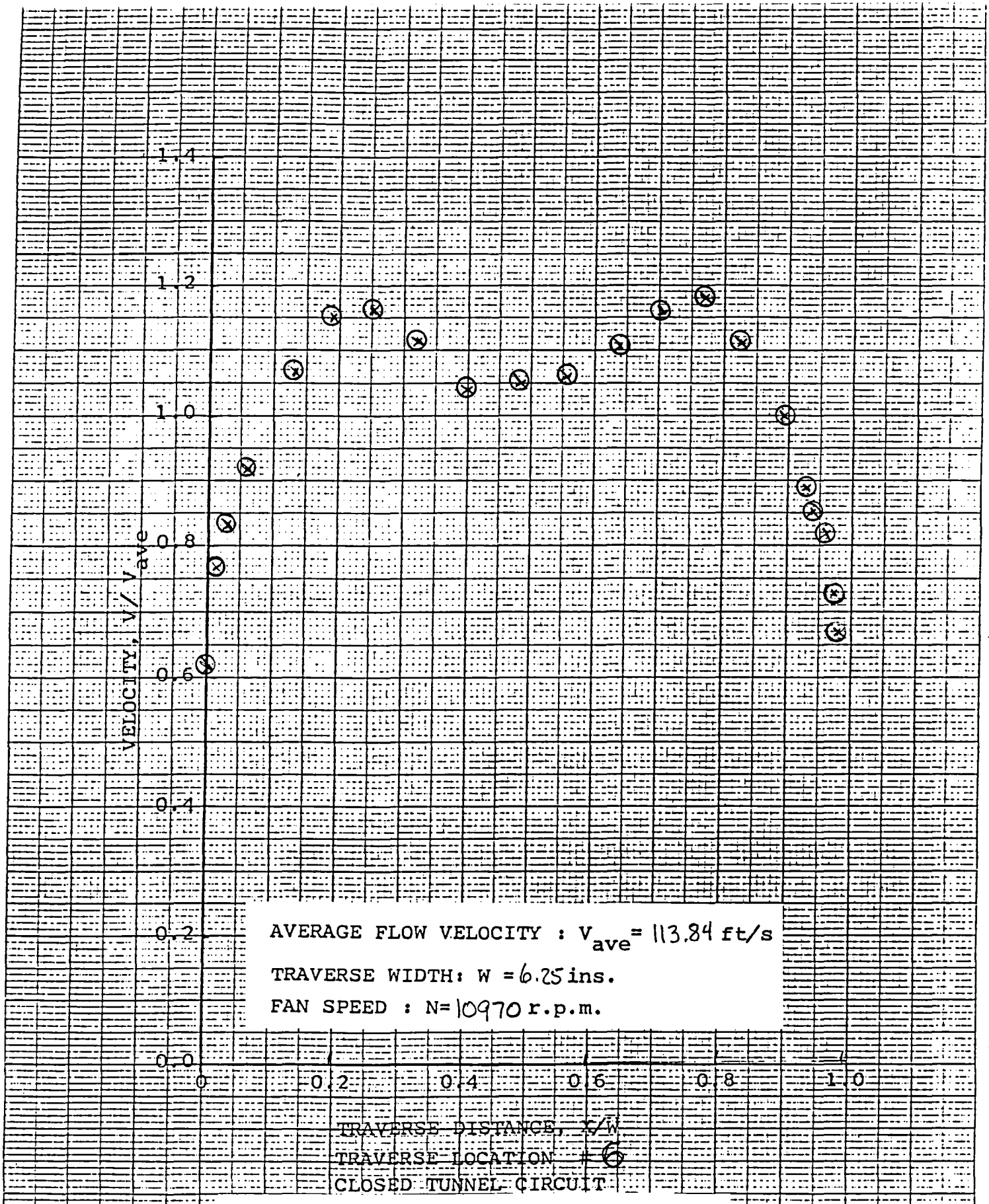

Figure 9f. Location #6

CONTINUED

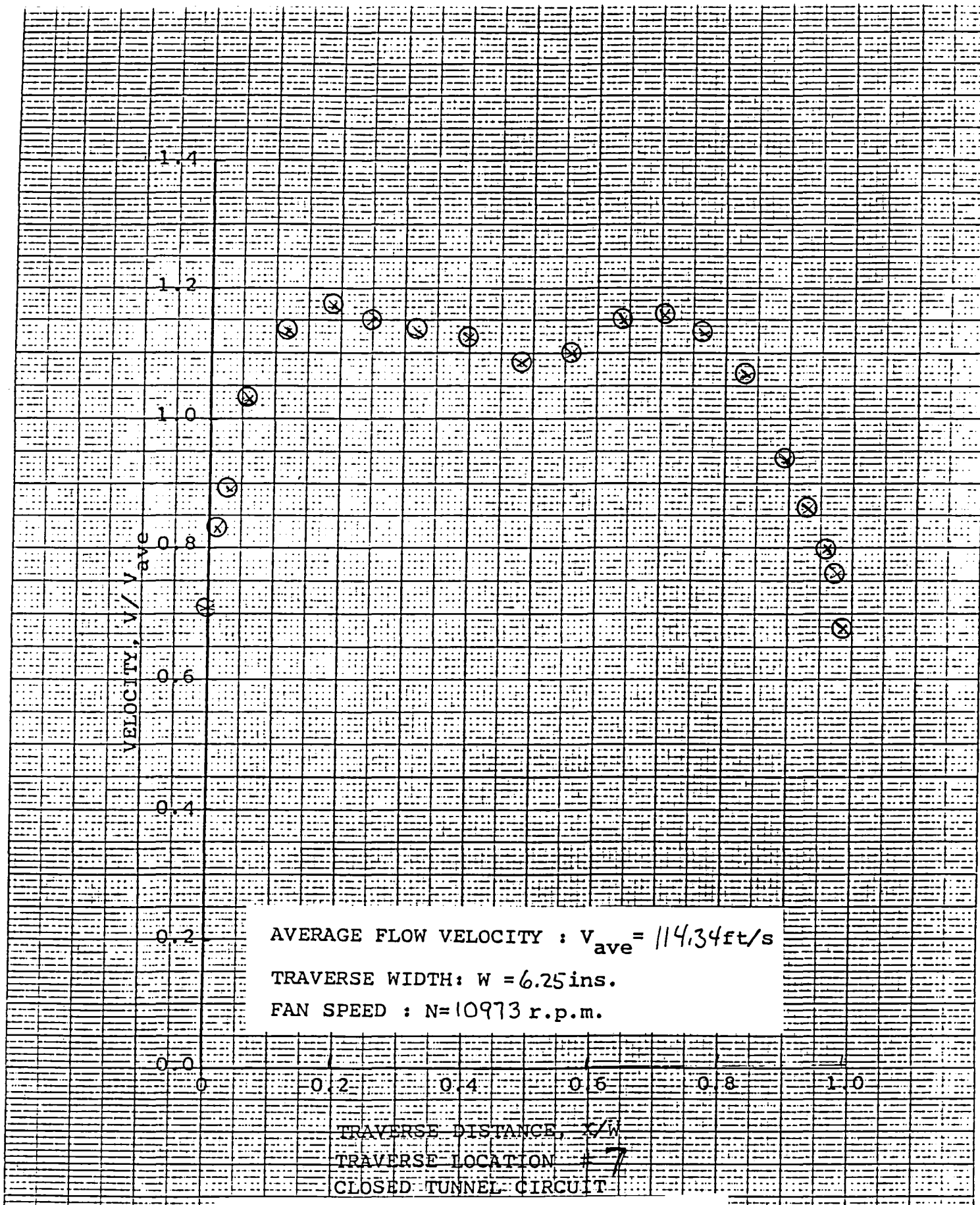

Figure 9g. Location #7
CONTINUED

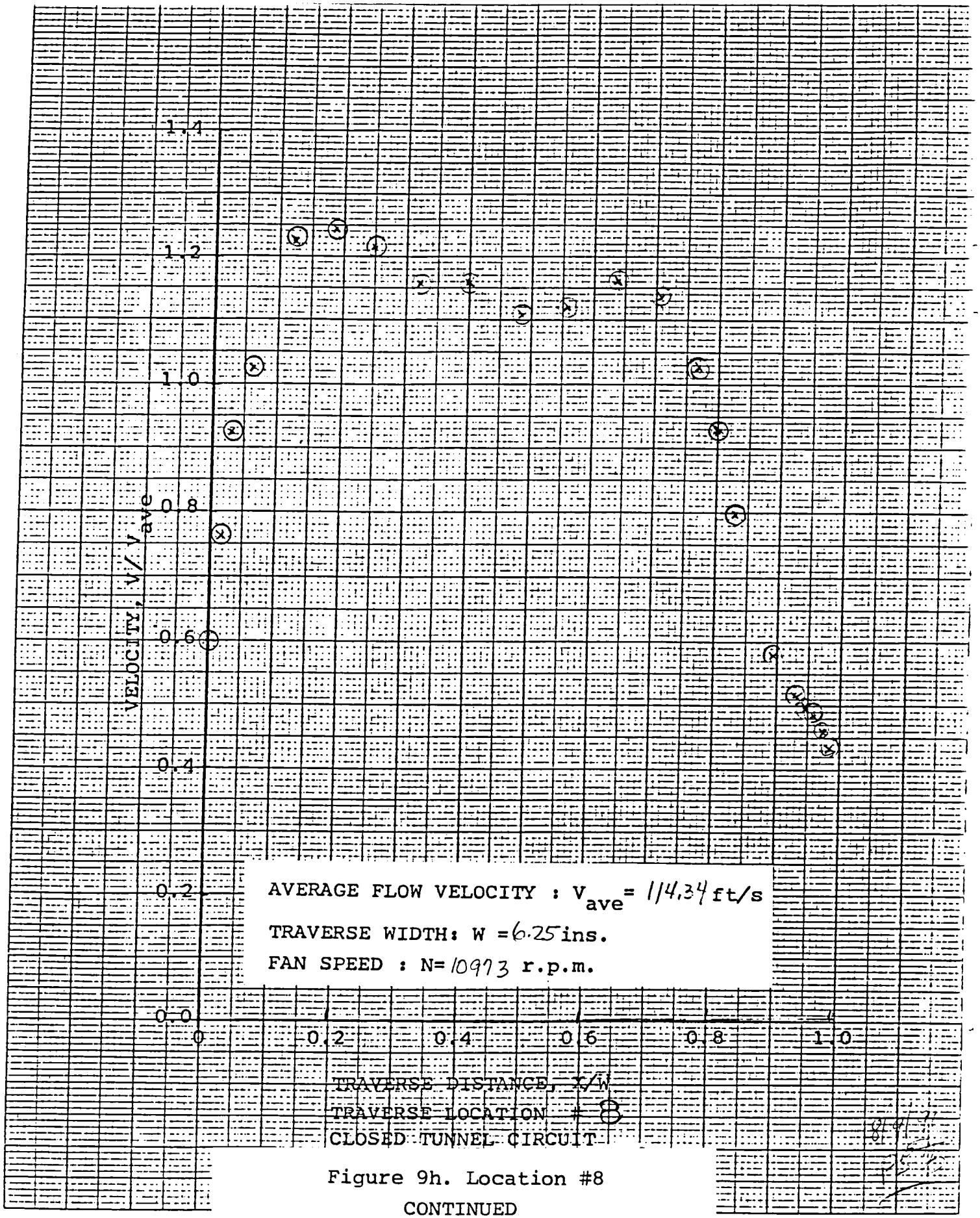

Figure 9h. Location #8
CONTINUED

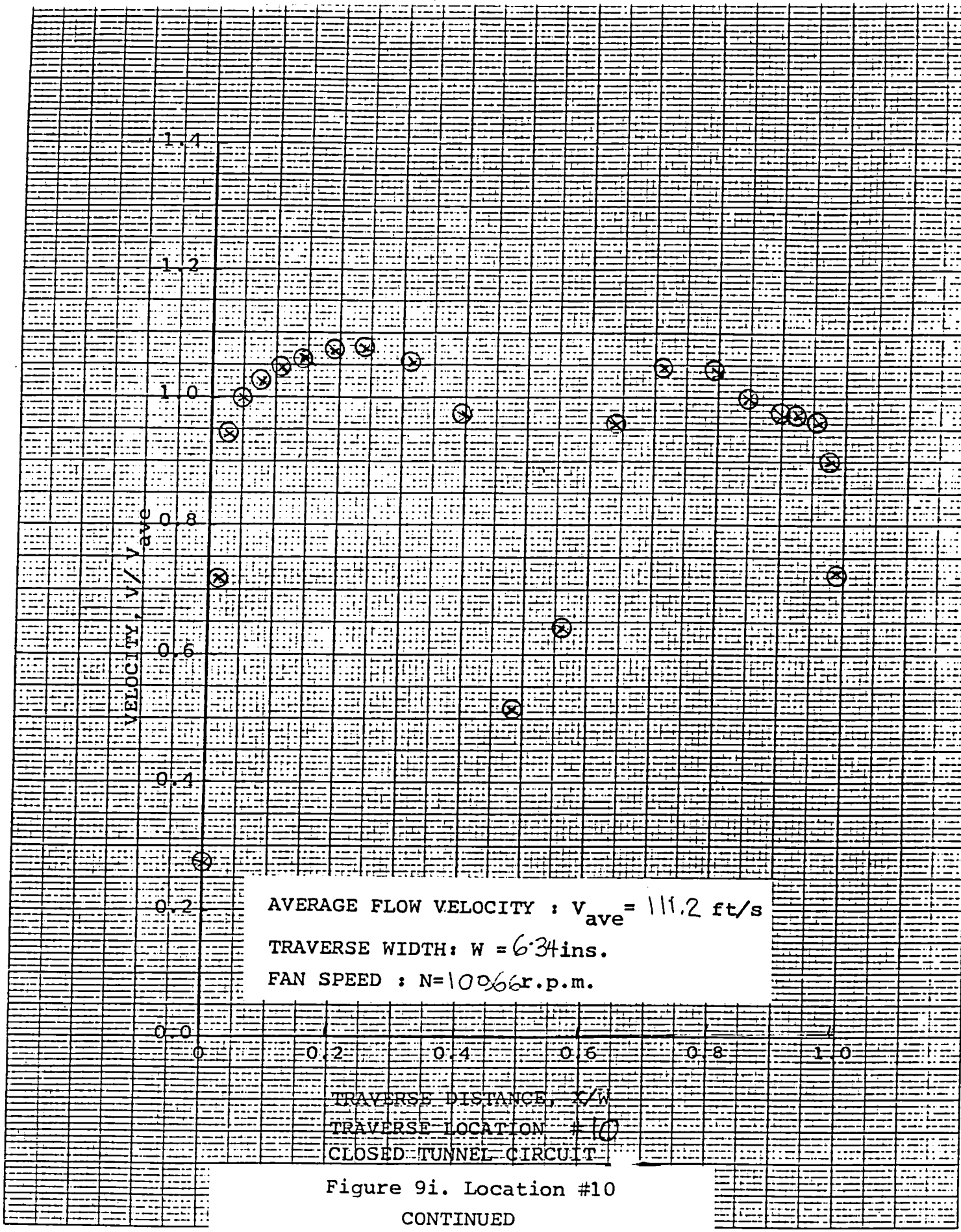

Figure 9i. Location #10
CONTINUED

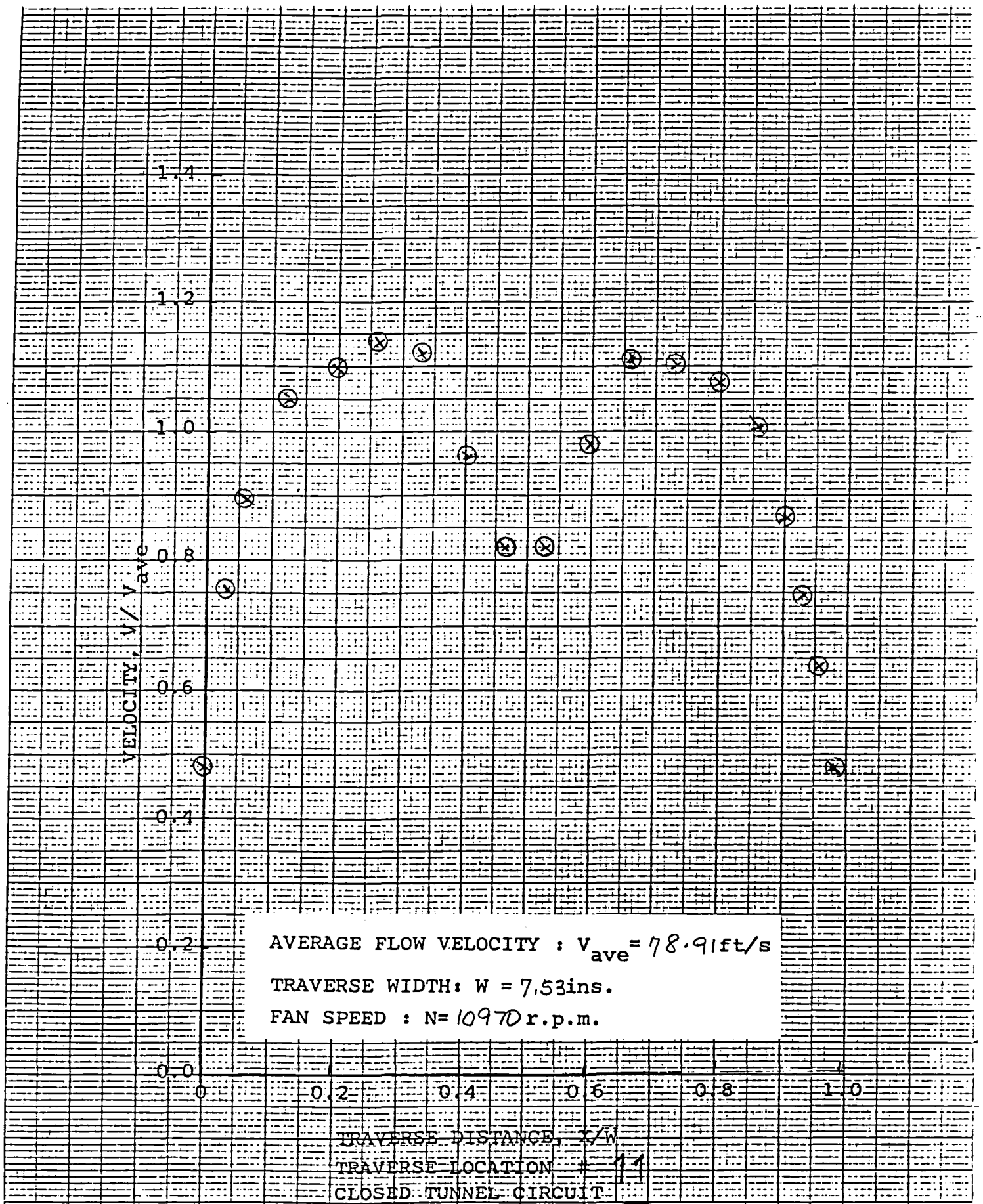

Figure 9j. Location #11

CONTINUED

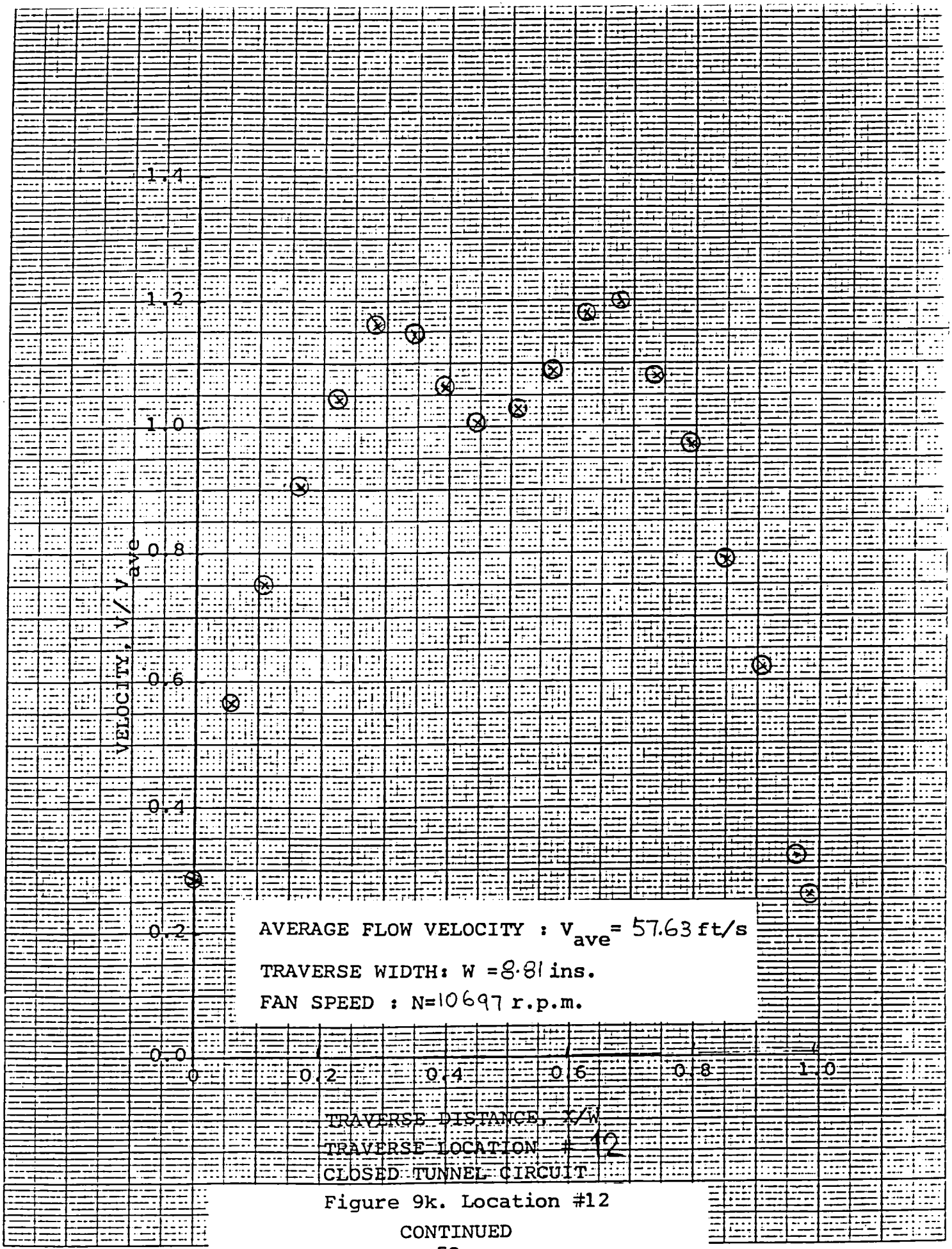

Figure 9k. Location #12

CONTINUED

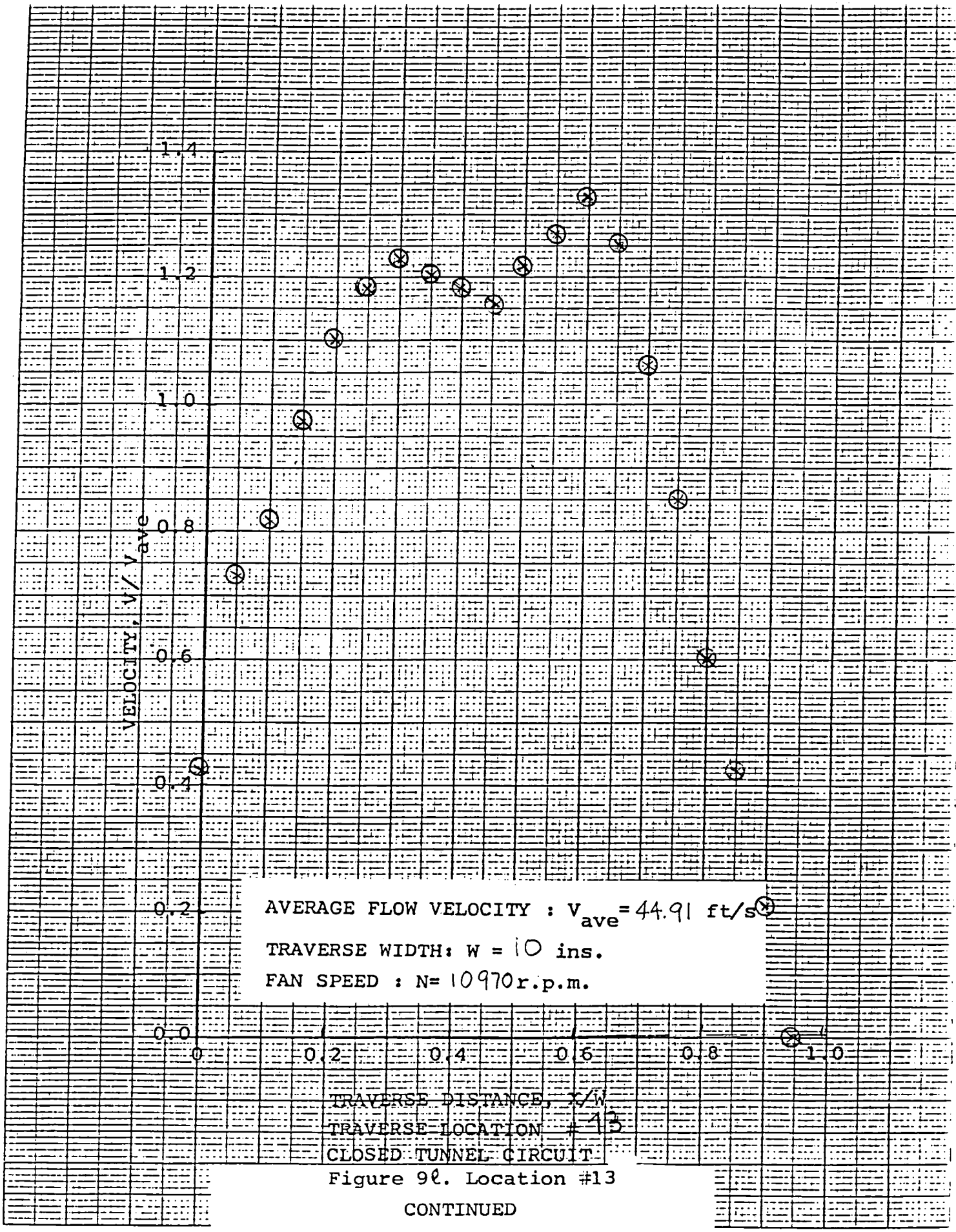

Figure 9ℓ. Location #13

CONTINUED

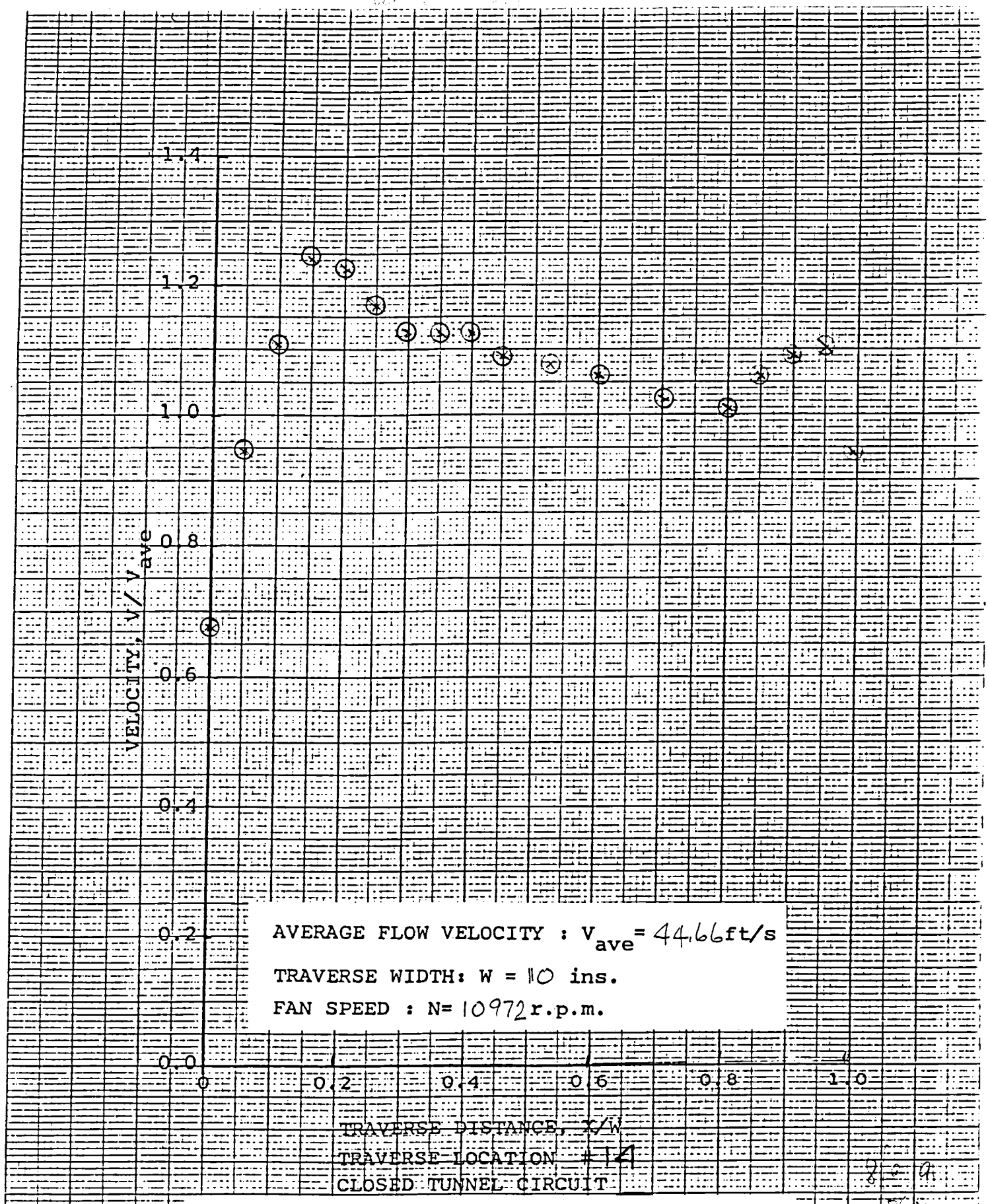

Figure 9m. Location #14
CONCLUDED

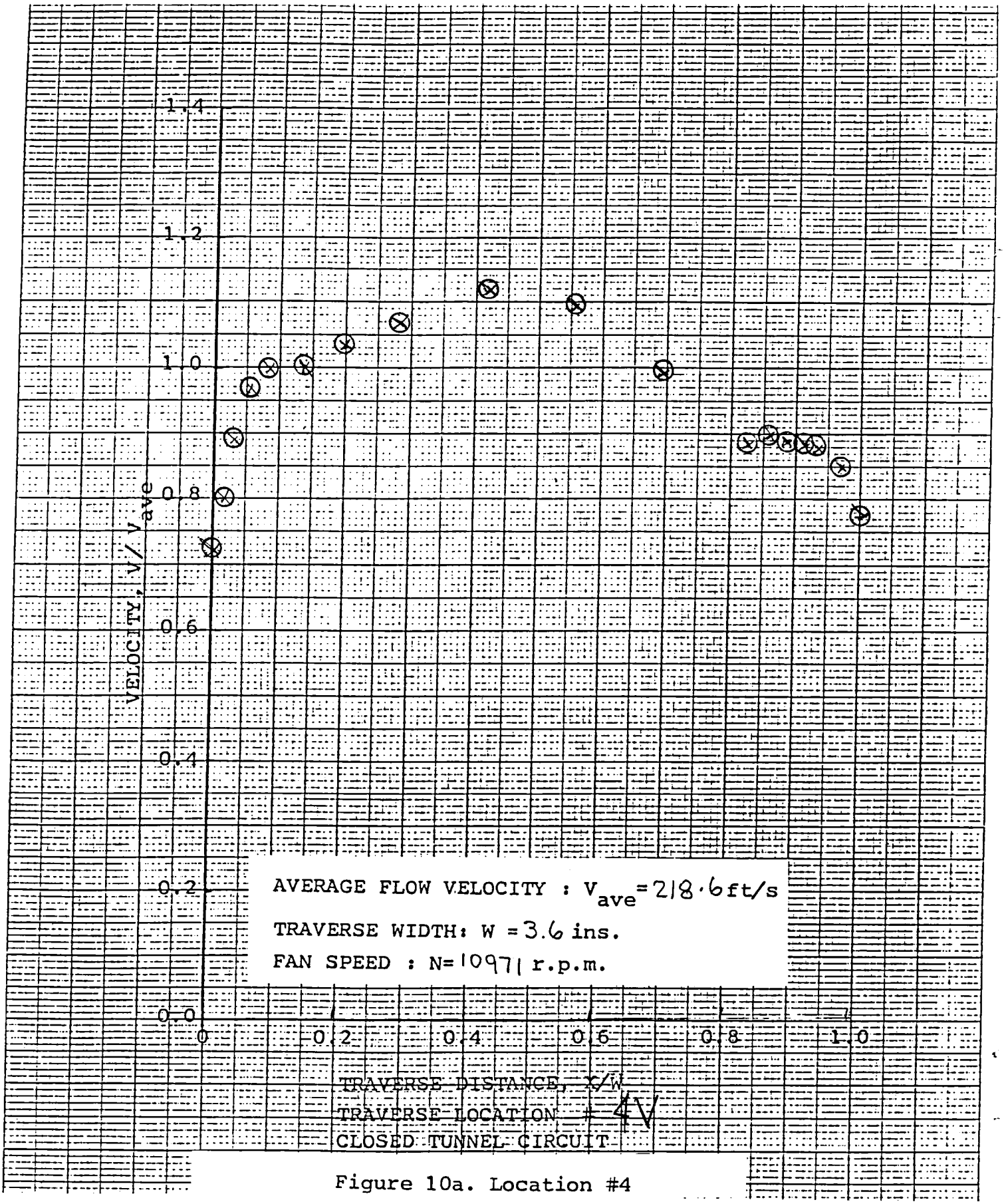

Figure 10a. Location #4

Figure 10. Vertical velocity traverses with the open test section.

CONTINUED

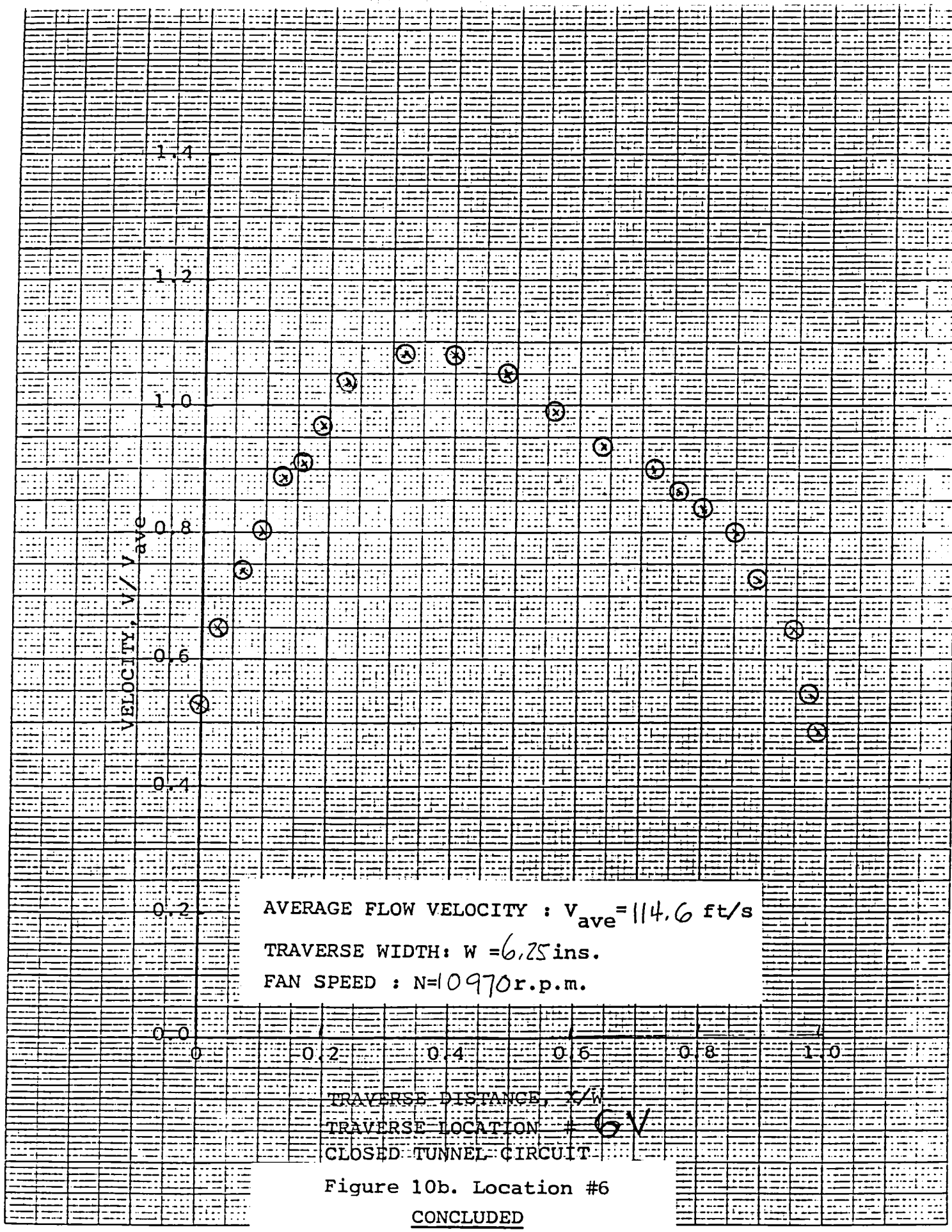

Figure 10b. Location #6
CONCLUDED

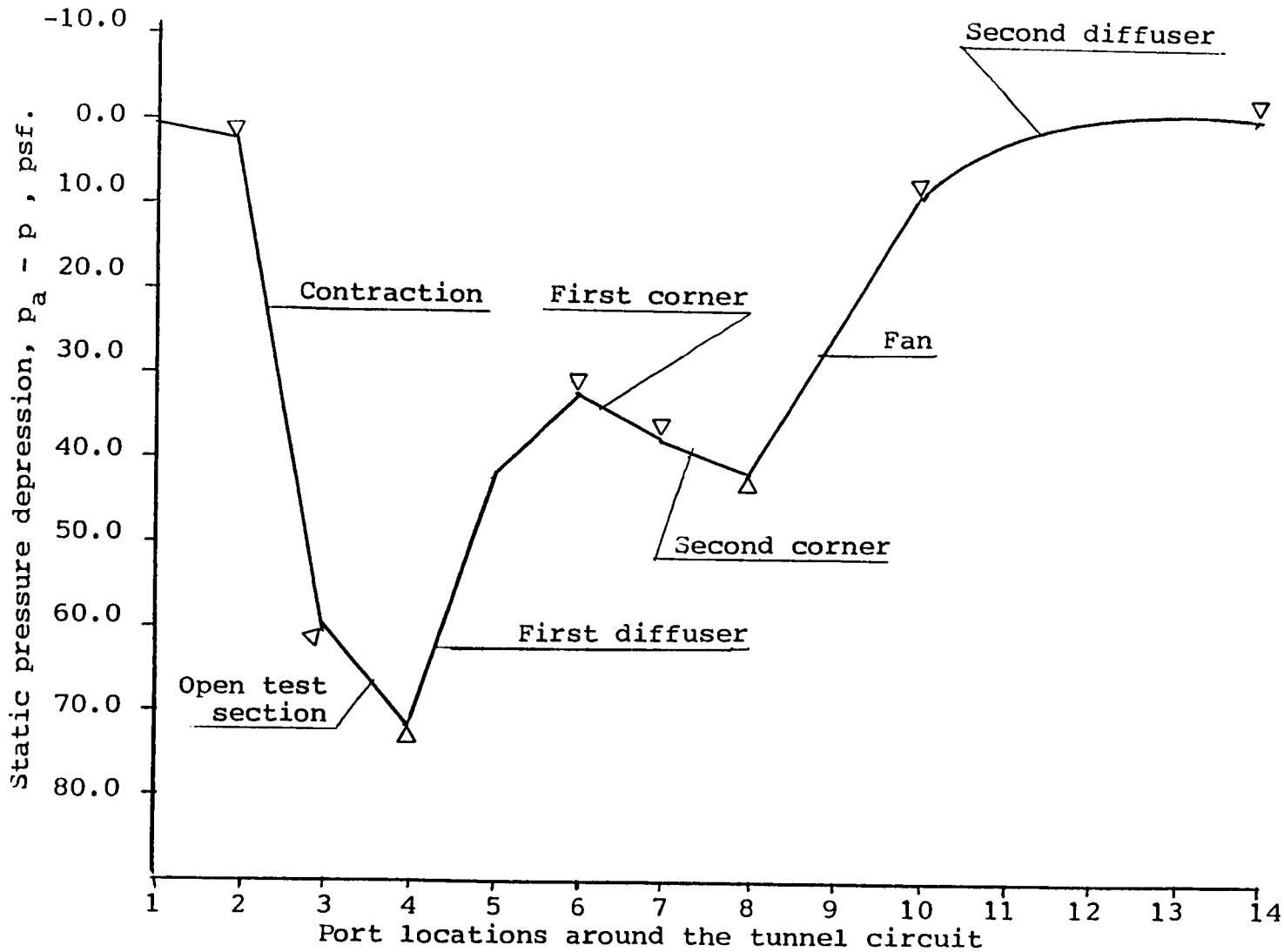

Figure 11. Pressure distribution around the circuit with the open test section

HORIZONTAL TRAVERSES

Traverse Location Number	Section Area Ft^2	Traverse Total Distance ins	CLOSED TEST SECTION Static Pressures psf p_2	p_3	Flow Rate Q ft^3/s	Average Section Velocity V_{ave} ft/s	OPEN TEST SECTION Static Pressures psf p_2	p_3	Flow Rate Q ft^3/s	Average Section Velocity V_{ave} ft/s
1	.545	10	3.3	67.9	25.90	47.53	2.8	59.7	24.31	44.60
2	.994	13.5	3.3	68.4	26.00	26.16	2.85	60.3	24.43	24.57
3	.1077 cts .136 ots	4.4 cts 5.11 ots	3.2	65.0	25.33	235.24	2.85	60.1	24.38	179.31
4	.110	4.4	3.3	67.9	25.43	231.26	2.70	58.3	24.03	223.10
5	.184	5.7	3.2	66.1	25.56	138.92	2.75	59.0	24.17	131.37
6	.213	6.25	3.3	68.0	25.92	121.70	2.9	59.5	24.25	113.84
7	.213	6.25	3.3	67.9	25.90	121.60	2.8	59.9	24.35	114.34
8	.213	6.25	3.3	67.3	25.80	121.05	2.8	59.9	24.35	114.34
10	.219	6.34	3.3	67.9	25.90	118.30	2.8	59.9	24.35	111.20
11	.309	7.53	3.1	67.9	25.94	83.90	2.75	59.9	24.36	78.91
12	.423	8.81	3.2	67.0	25.74	60.86	2.75	60.0	24.38	57.63
13	.545	10.0	3.2	67.9	25.92	47.53	2.80	60.45	24.47	44.91
14	.545	10.0	3.1	66.9	25.74	47.20	2.65	59.70	24.34	44.66

TABLE II: VERTICAL TRAVERSES

3V	.1077 cts .136 ots	3.6	3.2	65.3	25.39	235.8	-	-	-	-
4V	.110	3.6	3.2	65.5	25.43	231.26	2.8	58.5	24.05	218.6
6V	.213	6.25	3.1	66.7	25.70	120.67	2.8	60.2	24.42	114.6

Figure 12. Table I. Brief review of data

1/60 SCALE HSAWT PTS START-UP PROCEDURE

NOTE: TWO Operators are necessary to safely operate the PTS.

1. Turn on 100 Amp Breaker in MCC-2, 2CL for PTS Power. (Rm 150)
2. Turn on Breaker SII in PTS Power Supply. (Rm 154B)
3. Open air valve and water valve. Verify air flow for motor cooling and water flow for tunnel cooling.
4. Turn motor disconnect switch in the Reverberation Room to the "on" position.
5. Depress the "start" button on the motor starter in the Reverberation Room.
6. Turn on Master Key Switch #1 on PTS Control Panel.
7. Turn on Instrument Power Switch #3 on PTS Control Panel.
8. Turn on 115 VAC Switch #2 on PTS Control Panel.
9. Turn on Motor Control Switch #4 on PTS Control Panel.
10. Verify tunnel in Run Configuration. (Flanges tight, no loose parts in tunnel, etc.)
11. Verify RPM ADJ Pot at 0 00 on PTS Control Panel.
12. Push Reset Button on PTS Control Panel **TWICE**. Verify both halves of Motor Control light extinguish.
13. Preset initial motor start-up rpm by turning RPM ADJ to a set point of 3 00. This presents an initial propeller speed of approx. 2000 rpm.
14. Push RUN Button to Start Motor.
    CAUTION: At No Time should motor temperature exceed 250°F or tunnel air exceed 110°F.
15. Slowly bring fan up to predetermined rpm.
16. Monitor ALL three (3) temperature indicators, especially at high power and rpm levels.
17. Start-up for PTS complete—Enter on Log Sheet.

PTS EMERGENCY STOP PROCEDURE

IN THE EVENT OF AN EMERGENCY, PUSH THE RED MUSHROOM BUTTON. IMMEDIATELY BRING THE FAN SPEED CONTROL TO 0 00. THEN FOLLOW NORMAL SHUT DOWN PROCEDURE BEGINNING WITH STEP NO. 4.

NORMAL SHUT-DOWN PROCEDURE

1. Turn the RPM ADJ Pot counter-clockwise until the RPM reads zero.
2. When PROP stops, verify current on ALL phases is ZERO
3. Depress the "stop" button on the motor starter in the Reverberation Room.
   NOTE: Turning off the motor control switch # 4 also turns off the water flow for tunnel cooling.
4. Turn motor disconnect switch in the Reverberation Room to the "off" position.
5. Push the Red Mushroom button.
6. Turn the Motor Control Switch #4 Off.
7. Turn Off Breaker in PTS power supply. (Rm 154B)
8. Turn Off Breaker in MCC-2 2CL for PTS Power (Rm 150)
9. Turn Off 115 VAC #2, Instrument Power #3, and Master Key Switch #1.
10. Shut Down of PTS Complete—Enter on Log Sheet.
11. Close the air valve.

APPENDIX A

Procedures for start-up and shut down of the 1/60 scale model tunnel-

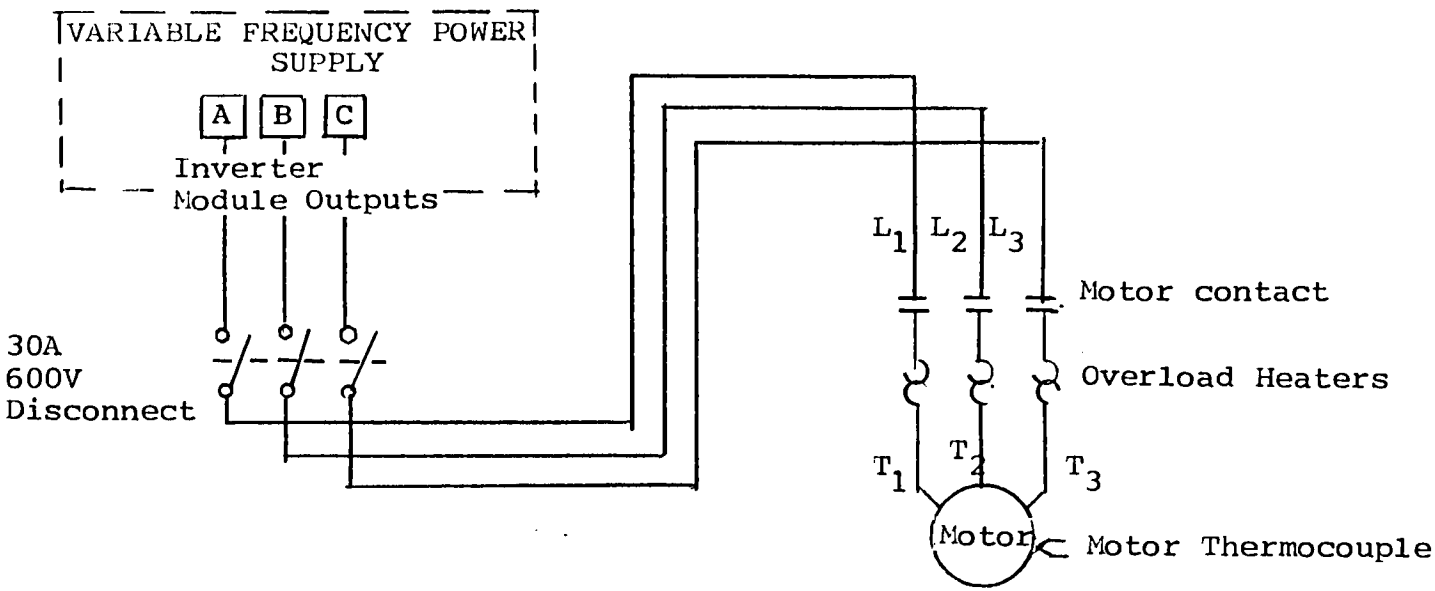

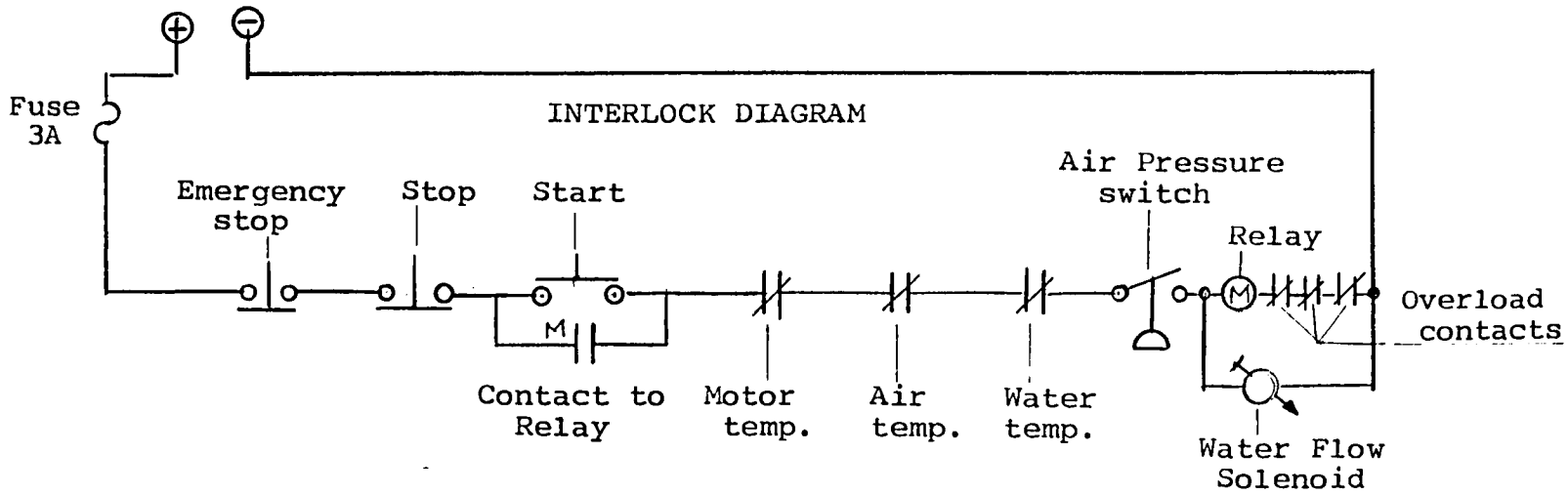

APPENDIX A

Figure A/1. Lay-out of the electric power line to the motor

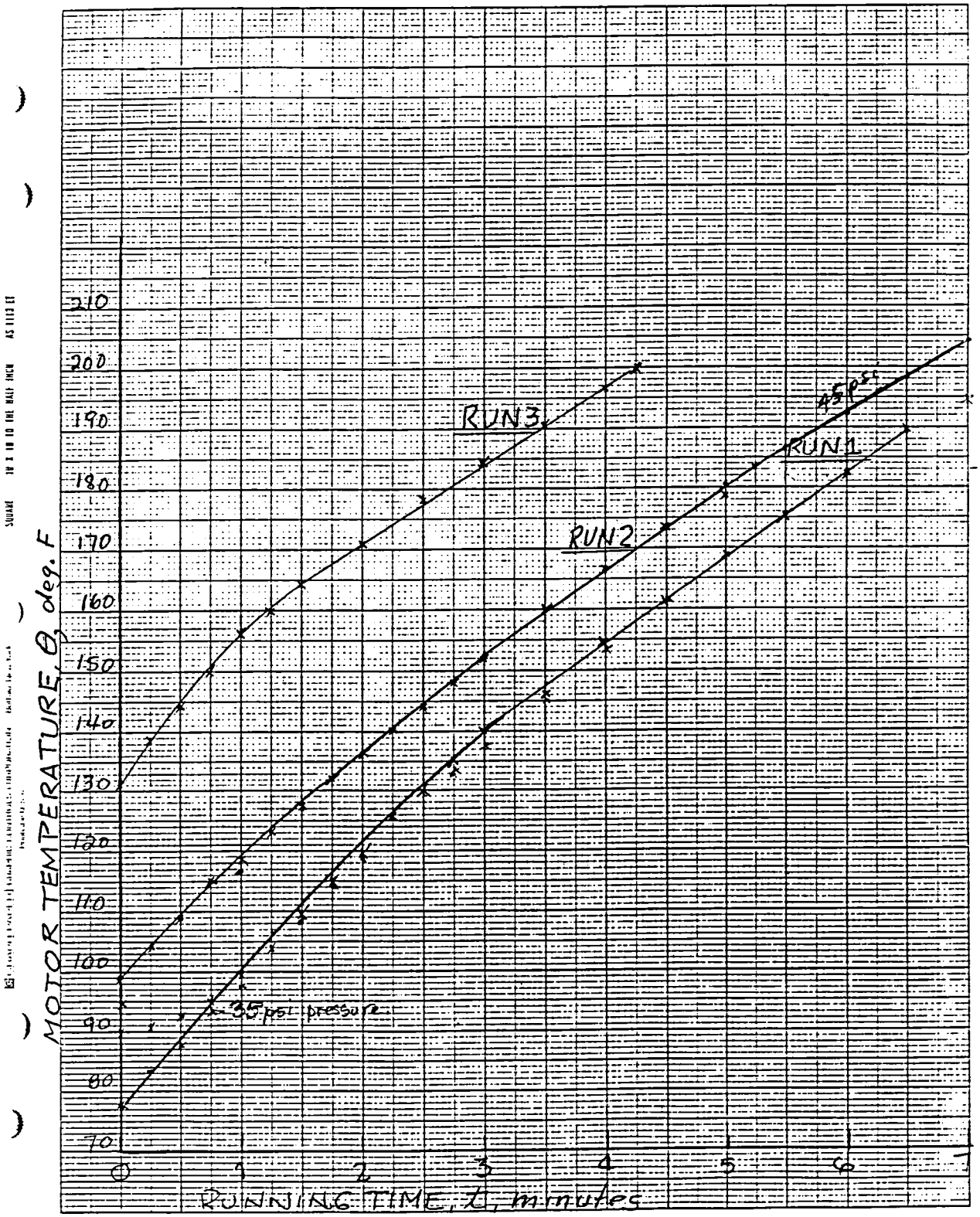

APPENDIX B

Figure B/1 . Variation of motor temperature with time, t , minutes

APPENDIX C

Pressure recovery in the diffusers.

CLOSED TEST SECTION:

Recovery will be defined by $R_d = \Delta p / q_{ave}$

Where Δp is the static pressure rise in the diffuser

$q_{ave} = 1/2\ \rho\ V_{ave}^2$

$V_{ave} = Q / A$, Q being the flow rate, A the cross area.

The flowrate Q was established from the pressure drop in the contraction, using 0.985 as coefficient and 0.0011 for density.

The $Q = 3.223 \sqrt{p_3 - p_2}$, where the pressures were obtained from the pressure distribution data.

First diffuser:

With $p_3 = 67.4$, $p_2 = 3.1$ p.s.f. Q= 25.84 cuft/sec, A=0.1077 ft^2

$V_{ave} = 25.84 / 0.1077 = 234.91$ ft/sec

$q_{av} = 1/2\ \rho\ V_{ave}^2 = 0.0011\ (234.91)^2 = 63.32$ psf.

The pressure rise was found $\Delta p = p_6 - p_4 = 67.1 - 29 = 38.1$

Hence for the first diffuser $R_{d1} = 38.1 / 63.32 = 0.6017 = 60.17\%$

Second diffuser:

The pressure rise was found $\Delta p = 10 - (-).6) = 10.6$ psf.

$V_{ave} = 25.84 /).213 = 121.31$ ft/sec, $q_{ave} = 16.19$ psf.

$R_{d2} = 10.6 / 16.19 =).6547 = 65.47\%$

****

OPEN TEST SECTION:

First diffuser

Calculations are similar. With p_3=60.45, p_2=2.8, Q=24.47 cuft/sec hence V_{ave} = 227.22 ft/sec , q= 56.78 psf. p = 71.43-33=38.43 psf.

Hence $R_{d1} = 38.43 / 56.78 = 0.677 = 67.7\%$

Second diffuser

With Q = 24.47 , $V_{ave} = 24.47/0.213 = 114.88$ ft/s, q_{ave}=14.52 and $\Delta p = 8.9 - (-0.5) = 9.4$ psf.

Hence $R_{d2} = 9.4 / 14.52 = 0.6475 = 64.75\%$

****

APPENDIX D

Calculation of the corner losses.

Loss will be defined by $C_p = p_{n+1} - p_n / q_{ave}$.

In this report the corner losses were calculated with the static pressure changes across the vanes rather than with the total pressure changes which is recognized as the more correct procedure. The main reason for this simplification was due to avoid the complex calculations because of the limited/available time/. It was intended to simply compare the corner loss of one set of vanes with the other, while the tunnel was operating either with the closed or with the open test section.

CLOSED TEST SECTION

First corner: $C_{p1} = p_7 - p_6 / q_{ave}$; where p_7=32.3 , p_6=29.0 psf. and q_{ave} = 16.19 psf.

Hence C_{p1} = 3.3 / 16.19 = 0.2038= 20.28%

Second corner: $C_{p2} = p_8 - p_7 / q_{ave}$, where p_8 = 37.3 psf.

Hence C_{p2} = 5.0/ 16.19 =0.3088= 30.88%

OPEN TEST SECTION

First corner: p_7 = 37.75 , p_6 = 33 psf. q_{ave}= 14.52 psf.

Hence C_{p1} = 4.75 / 14.52 = 0.327= 32.7%

Second corner : p_8 = 42.2

Hence C_{p2}= 4.45 / 14.52 = 0.3065= 30.65%